University of Central Florida

STARS

2020

Gelsolin-Mediated Actin Filament Severing in Crowded Environments

James Heidings
University of Central Florida

GELSOLIN-MEDIATED ACTIN FILAMENT SEVERING IN CROWDED ENVIRONEMNTS

By

JAMES B. HEIDINGS

B.S. University of Central Florida, 2018

A thesis submitted in partial fulfillment of the requirements
for the degree of Master of Science
in the Burnett School of Biomedical Sciences
in the College of Medicine
at the University of Central Florida
Orlando, Florida

Summer Term
2020

Major Professor: Ellen Hyeran Kang

ABSTRACT

Actin is an essential cytoskeletal protein that plays key roles in several cellular functions such as phagocytosis and cell motility with the help of actin binding proteins (ABPs). Gelsolin is a calcium regulated ABP that severs and caps actin filaments. Gelsolin helps control actin filament assembly dynamics that are required for cell survival. Cleavage products of gelsolin lead to Familial Amyloidosis, Finnish type, and conformational changes to gelsolin are implicated in disease progression. The majority of in vitro studies of gelsolin and actin have been performed in dilute buffer conditions which do not simulate the molecular interactions occurring in the intracellular environment. The intracellular space is packed with many macromolecules such as carbohydrates and other proteins. These macromolecules induce steric hindrance and excluded volume effects and have been shown to alter protein-protein interactions and protein conformations. We hypothesize that gelsolin and actin filaments present in crowded environments will produce greater gelsolin severing activity due to steric hinderance and induced conformational changes. To test this hypothesis, we have visualized actin filament severing by gelsolin in solution with macromolecular crowders utilizing total internal reflection fluorescence (TIRF) microscopy. Steady-state average filament lengths and filament length distributions were analyzed to determine the effect crowding has on gelsolin-mediated filament severing. Real-time filament severing assays visualized by TIRF allowed us to compare gelsolin's severing efficiency in the presence of crowders to those in dilute buffer conditions. Co-sedimentation assays were performed in order to determine the effect of crowding on gelsolin binding to actin filaments. Taken together, this study demonstrates that macromolecular crowding modulates gelsolin-mediated actin filament severing activities, offering insights into the interactions between actin and gelsolin inside the cell. These

insights will deepen our understanding of in vivo cytoskeletal regulation which is linked to cell physiology and may aid researchers studying actin-related diseases.

ACKNOWLEDGEMENTS

TABLE OF CONTENTS

LIST OF FIGURES

LIST OF TABLES

LIST OF ACRONYMS

3D	Three Dimensional
ABP	Actin Binding Protein
ADP	Adenosine Di-Phosphate
ADP + Pi	Adenosine Di-Phosphate + Phosphate
Arp2/3	Actin Related Protein 2/3
ATP	Adenosine Tri-Phosphate
BSA	Bovine Serum Albumin
ddH$_2$O	Double Deionized Water
DTT	Dithiothreitol
EGTA	Ethylene Glycol-bis(β-aminoethyl ether)-N,N,N',N'-Tetraacetic Acid
F-actin	Filamentous Actin
FAF	Familial Amyloidosis, Finnish-Type
G-actin	Globular Actin
KMI	Potassium Magnesium Imidazole
kDa	Kilodalton
m/V	Mass by Volume
PAGE	Polyacrylamide Gel Electrophoresis
PIP$_2$	phosphatidylinositol 4,5-bisphosphate
PEG	Polyethylene Glycol
sX	Gelsolin Segment X
SDS	Sodium Dodecyl Sulfate
SE	Standard Error
SEM	Standard Error of the Mean
STDEV	Standard Deviation
t_1	Decay Time Constant
TIRF	Total Internal Reflection Fluorescence
v/v	Volume by Volume
w	Width

w/v   Weight by Volume

w/w   Weight by Weight

CHAPTER ONE: INTRODUCTION

Chapter one focuses on background information about the concepts and proteins described in this thesis. I will describe actin's role in the cytoskeleton, the role of gelsolin in the cell and specifically in relation to actin severing, and finally I will discuss macromolecular crowding.

1.1 The Cytoskeleton

1.1.1 The Actin Cytoskeleton

Actin is an essential cytoskeletal protein that is involved in cardiac muscle contraction[1], maintenance of cell shape[2], generation of force for migration[3], and phagocytosis[4]. Changes in average actin filament lengths and polymerization rates have been associated with changes in cellular motility[5], shape[6], and apoptosis[7, 8]. These processes are controlled by actin binding proteins such as actin related protein 2/3 (Arp2/3) complex, gelsolin, cofilin, and profilin. Studying actin filament length and polymerization kinetics in various conditions or in solution with pharmaceutical compounds offers researchers insight into the molecular mechanisms that cause or prevent disease states and the processes that enable cell movement.

Actin is found in the cell in monomeric and polymeric forms. Monomeric actin, or G-actin, is the globular form, which self-assembles to form a nucleus. This actin nucleus can then elongate into actin filaments under physiological ionic conditions. G-actin is a 42 kDa protein and is made up of 4 subdomains with a nucleotide-binding cleft.[9] Polymeric actin, or F-actin, is the filamentous form of actin. In order to form an actin filament, two to three actin monomers must non-covalently associate and form a nucleus.[10-12] From this actin nucleus, monomers can be reversibly added to

the filament. Actin filaments form a double helix structure and have polarity **(Fig. 1)**.[9] These actin filaments have several functions within the cell, one of them being force generation for motility. When required, actin polymerizes at the leading edge of the cell with the help of actin binding proteins (ABPs). This action can create structures that protrude from the cell such as lamellipodia.[13] Once the lamellipodia has grown a sufficient distance, the cell will create focal adhesion points with the substrate, and old adhesion points at the trailing end of the cell are disassembled.[14] One side of the filament is the barbed or (+)-end to which new ATP-actin monomers are rapidly added, and the other end of the filament is the pointed or (-)-end from which ADP-actin monomers dissociate. During elongation of the actin filament, actin monomers join either end of the filament at roughly the same rate, however, once the filament reaches steady state ATP-actin monomers join the barbed end at the same rate as ADP-actin monomers leaving the filament from the pointed end **(Fig. 2)**.[9] At this point the filament is in the steady state, and there is no net change in the filament length.

The process of actin filament assembly and disassembly is dynamic in living cells, and due to the myriad of functions actin filaments serve, the cell requires several ways to regulate actin polymerization kinetics. Under physiological conditions ATP-G-actin will polymerize into ATP-F-actin, which is energetically favorable.[9] Overtime, the ATP-F-actin hydrolyzes to ADP-F-actin, and because ADP-G-actin is more stable than ADP-F-actin the monomer will dissociate from the pointed end of the filament. The pH of the environment also has an effect on actin nucleation and polymerization.[15] At low pH the rate of actin polymerization is increased, and the critical concentration, which is the concentration that G-actin is in equilibrium with F-actin, is increased.[16] Ionic interactions also help control actin filament assembly and mechanics.[17] For example,

monovalent cations (e.g., KCl) or divalent cations (e.g., MgCl$_2$) can bind to actin and cause increases in the polymerization rate[18] and enhance filament stiffness[17]. Another way the cell modulates actin kinetics is by the use of ABPs. There are many actin binding proteins with various functions. The Arp2/3 complex for instance is able to nucleate new daughter filaments.[19] Gelsolin, is an important ABP which severs actin filaments and subsequently caps the barbed end, stopping elongation of the filament. Gelsolin will be the focus of this thesis.

Actin has been implicated in several different disease states. For instance, actin expression is changed after a myocardial infarction in surviving myocytes[20], which researchers propose effects disease progression[21]. Mutations in the gene that codes for alpha-muscle actin, ACTA1, can lead to congenital myopathies that lead to infant death.[22] These mutations are also believed to cause about 20% of nemaline myopathy.[23] Nemaline myopathy is characterized by the presence of thread-like or rod-like structures called "nemaline bodies" and are observed in patient muscle biopsies. Myopathies such as this can lead to difficulty breathing, insufficient heart function, and general muscle weakness. Some mutations in the ACTA1 gene can produce changes to the structure of actin, which is hypothesized to disrupt actin kinetics and binding.[24, 25]

1.1.2 Gelsolin

Gelsolin is an 86 kDa 6-segment (s1-s6) protein[26] **(Fig. 3)** that is able to cleave actin filaments and cap them on the barbed end, in the presence of calcium (Ca^{2+}), preventing monomer addition of the cleaved filament **(Fig 4)**.[27, 28] This can lead to disassembly of the actin filament. Gelsolin s1 and s4-s6 contain the G-actin binding sites, while s2-s3 have the highest affinity F-actin binding sites.[28] At low calcium concentrations gelsolin is in a conformation unable to bind

to F-actin. There is a two-step activation process, one occurring at 0.1-5 µM Ca^{2+} and a second at 10 µM-1 mM Ca^{2+} concentrations.[29] The currently proposed mechanism for gelsolin severing begins with activated gelsolin binding to F-actin via the s2 subdomain. This allows s1 to also bind to the filament tightly. The s1 subdomain then weakens the non-covalent inter-subunit interactions, thus severing the filament. After severing, gelsolin caps the filament on the barbed end.[28] As a mechanism of fine control over actin kinetics, after cleavage gelsolin can be removed from the barbed end by cellular signals such as phosphatidylinositol 4,5-bisphosphate (PIP_2).[30] After severing filaments and being removed as a cap by PIP_2, gelsolin severing yields two barbed ends, both of which can polymerize, effectively doubling the amount of actin polymerization. While this project focused on the severing activity of gelsolin, the protein has several other functions inside the cell such as mediating cytoskeletal reorganization for cellular migration.[31]

Gelsolin plays a key role in cellular locomotion by controlling actin polymerization and disassembly at the leading edge of the cell.[10] Gelsolin has been shown to be diffuse throughout the cytoplasm as well as localize at actin stress fibers and cell edges.[32] Gelsolin's localization at the cell edge gives gelsolin the opportunity to rapidly sever and remodel the cytoskeleton, leading to force generation needed for migration.[33] Studies have shown that cellular motility is enhanced in fibroblast cells when gelsolin is overexpressed[33], while other have demonstrated that by knocking out gelsolin, platelet shape changes occur less often, and fibroblasts migrate slower[34]. As demonstrated by the aforementioned studies gelsolin-mediated cytoskeletal rearrangements are needed for proper cellular motility.

Gelsolin is able to nucleate actin polymerization by binding to two actin monomers, stabilizing their interaction.[29] This process leads to greater actin polymerization by skipping the

initial lag phase that occurs in spontaneous polymerization. Gelsolin also plays a role in cellular apoptosis, or programed cell death. Under certain conditions, such as hypoxia, caspase-3 can cleave gelsolin, producing two halves of the protein, an N-terminal and a C-terminal half. The N-terminal half of the protein is then able to release DNase1 from a gelsolin:actin:DNase1 complex present in the cytoplasm. The released DNase1 is then free to enter the nucleus and induce apoptosis.[28] In addition, full-length gelsolin can act to inhibit cellular apoptosis by suppressing the release of cytochrome c, an apoptotic factor, from the mitochondria.

Changes in gelsolin function and expression have been associated with several diseases, including cardiovascular diseases[35, 36] and Familial Amyloidosis, Finnish-type (FAF) also known as gelsolin amyloidosis. In FAF, aberrant cleavage of gelsolin leads to the deposition of small fragments that form plaques in the nerves of the face. This leads to facial paralysis and the formation of cataracts.[37] Gelsolin is also active in caspase-mediated apoptosis, which involves drastic cytoskeletal rearrangement. When caspase 3 cleaves gelsolin, the N-terminal of gelsolin is also able to bind and sever filamentous actin independent of calcium, and leads to rapid actin disassembly which is an important step in myocardial apoptosis.[38, 39]

1.2 Macromolecular Crowding

Macromolecular crowding refers to the physical effects generated by large, inert macromolecules in solution. Macromolecular crowding has been shown to cause variations in protein-protein interactions[40], and changes to protein structure[41, 42]. The intracellular space has been found to be very crowded, with up to 40% of the available space in the cytoplasm occupied (**Fig. 5**).[43] High volume occupancy inside cells brings about an excluded volume effect, which

effectively increases the concentration of solutes by reducing the intracellular volume available.[44] The conformational changes in proteins caused by macromolecular crowders may affect protein-protein interactions, such as those between actin and gelsolin.

Most *in vitro* analysis of actin and gelsolin has been performed in dilute buffer conditions. These conditions, however, do not properly model the intracellular environment, which is packed full of macromolecules and proteins. Projects from other groups have found that macromolecular crowding drastically increases actin polymerization rate, leads to the production of more filaments, and reduces the critical concentration.[45] It has also been shown that molecular crowders stabilize actin[46] and slow G-actin unfolding[47]. Based on these findings it is clear that the macromolecular effects present inside the cell should be considered by biophysicists during the study of ABPs and actin.

Castaneda et al. has recently demonstrated that macromolecular crowding promotes enhanced filament mechanics and conformational changes in actin filaments. In crowded environments, actin filaments are shorter and stiffer on average and an over-twist of the double helical structure occurs.[48, 49] Filament over-twisting may alter ABP binding interactions. For example, changes in filament twist have shown to modulate the binding and severing activity of cofilin.[50, 51] Gelsolin may act similarly to cofilin when interacting with the over-twisted filaments. A computational study recently published by Lee and Kang found that gelsolin segment-1 (s1) has altered binding to the barbed end of actin filaments depending on the conformation of the filament.[52] Other studies have suggested that macromolecular crowding decreases enzymatic activity.[53] The function of gelsolin severing in crowded environments has not been studied, but the

6

mentioned studies imply that gelsolin's severing activity may also be modified by macromolecular crowding.

1.3 Motivation

Gelsolin's activity and expression levels have been found to be involved in myocardial infarctions in several cellular studies.[21, 35, 54] In some cases of FAF, a single nucleotide polymorphism causes a change in the conformation of gelsolin. This change in shape allows aberrant furin cleavage, which is the first step in plaque formation.[55] Understanding the effect intracellular crowding on gelsolin's function may offer insight into gelsolin related diseases. Extracellular studies of gelsolin have focused mainly on characterizing actin severing activity.[27, 56-60] These experiments have been performed extensively and provide a good understanding of gelsolin's mechanics in dilute buffer conditions. In order to model and consider the effects of a crowded intracellular environment, we characterized gelsolin's actin severing activity in solutions crowded with inert macromolecular crowders. The crowders used for this project were sucrose, which is an inert sugar molecule, and polyethylene glycol (PEG), which is an inert macromolecular polymeric crowder. We hypothesized that gelsolin and actin filaments present in crowded environments would lead to greater severing activity due to steric hinderance and the excluded volume effects. To date the majority of actin binding protein studies have been performed in dilute buffer conditions, thereby providing an imperfect understanding of their function inside the cell. Taking into consideration the effect intracellular crowding has on gelsolin may offer insight into various diseases such as FAF.
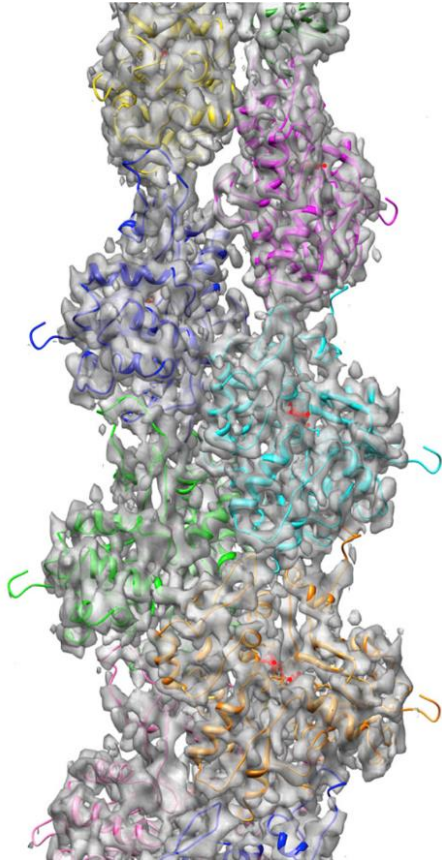
Figure 1: 3D Reconstruction of frozen hydrated actin filaments.

Stereo view with 4.7Å resolution. Copyright permission obtained from Elsevier, 2020.[61]
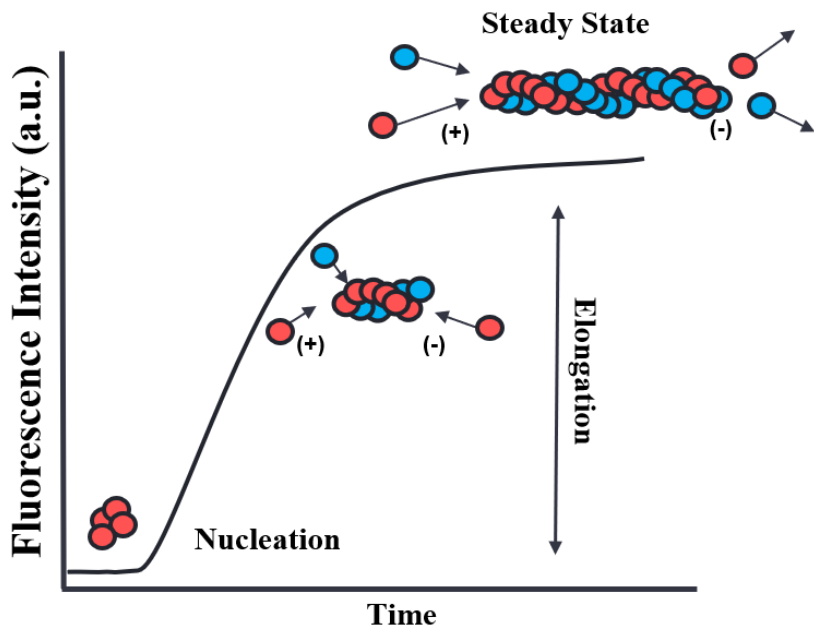
Figure 2: Polymerization of actin measured through fluorescence intensity.

After an initial nucleation phase the filament enters the elongation phase where monomers add to the barbed (+)-end and the pointed (-)-end at the same rate. Finally the filament reaches the steady state where the same number of monomers associate at the (+) end as dissociate at the (-) end.
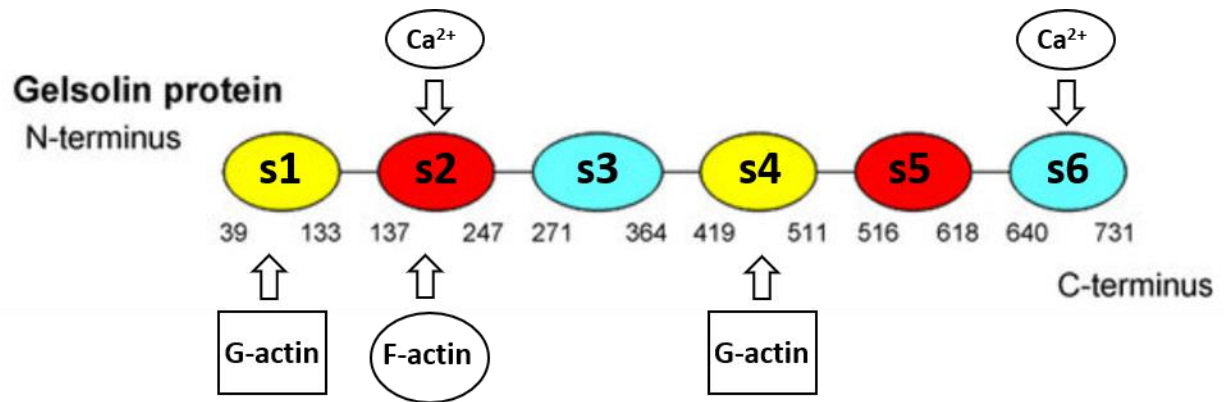
Figure 3: Cartoon representation of gelsolin.

G-actin, F-actin, and calcium binding sites specified. Copyright permission obtained from Elsevier, 2020.[62]
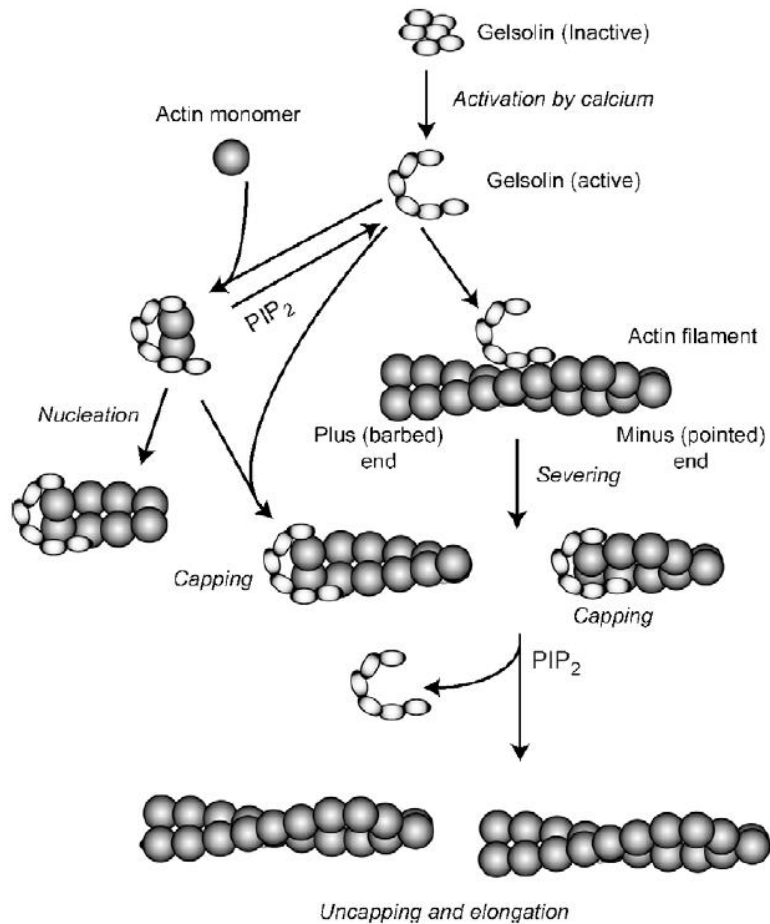
Figure 4: Cartoon representation of gelsolin function.

On the left gelsolin function as a nucleation factor is depicted. Gelsolin can sequester and stabilize several actin monomers, producing an actin nucleus for polymerization. On the right gelsolin severing activity is depicted. When activated gelsolin binds to F-actin it weakens non-covalent bonds between actin monomers, leading to filament severing. Gelsolin then caps the barbed end of the filament. Copyright permission obtained from Elsevier, 2020.[63]
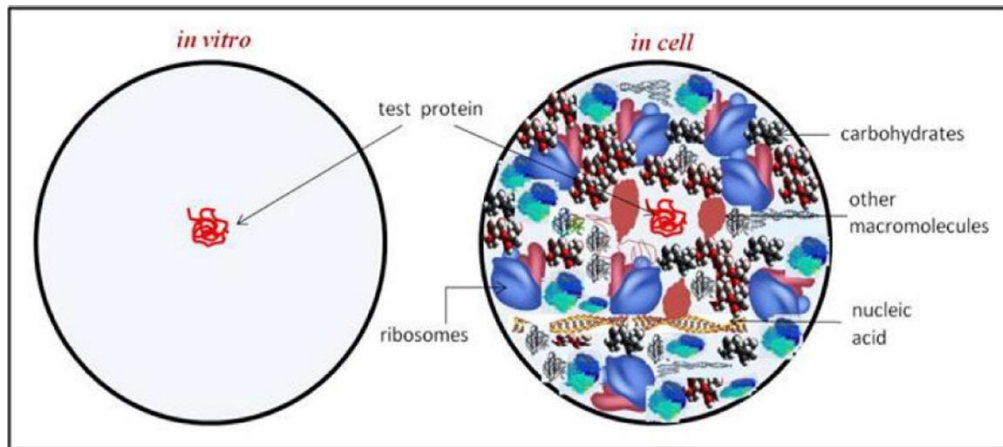
Figure 5: Cartoon representation of a test protein in dilute buffer conditions (left) and inside the cell (right).

The intracellular space is packed with high concentrations of macromolecules such as carbohydrates, nucleic acids, and ribosomes. Copyright permission obtained from Elsevier, 2020.[64]

CHAPTER TWO: MATERIALS AND METHODS

2.1 Actin Purification and Sample Preparations

Unlabeled actin was purified from rabbit skeletal muscle acetone powder (Pel-Freeze Biologicals Inc., Rogers, AR) , subsequently filtered through a Sephacryl S-300 size exclusion column equilibrated in buffer-A (2 mM Tris-HCl, pH 8.0, 0.2 mM $CaCl_2$, 1 mM NaN_3, 0.2 mM adenosine 5-triphosphate (ATP), and 0.5 mM dithiothreitol (DTT)) as described in Kang et al.[17] Labeled (pyrene, rhodamine, and biotin) rabbit skeletal muscle actin (>99% purity) proteins were purchased from Cytoskeleton Inc. (Denver, CO) and stored in buffer-A. A cation exchange was performed on calcium bound G-actin to replace Ca^{2+} with Mg^{2+}, equal to the concentration of G-actin plus 10 µM, and with Ethylene glycol-bis (β-aminoethyl ether)-N,N,N',N'-tetraacetic acid (EGTA, 0.2 mM). Actin polymerization was initiated by the addition of $1/10^{th}$ volume 10x polymerization buffer (10 mM ATP, 10 mM DTT, 100 mM imidazole, 2 mM $CaCl_2$ pH 7.0, 500 mM KCl, 20 mM $MgCl_2$). Human recombinant plasma gelsolin was purchased from Cytoskeleton Inc. (Denver, CO) and stored in gelsolin buffer (10 mM Tris, 10 mM NaCl, 0.1 mM $MgCl_2$, 1% w/v sucrose, and 0.1% w/v dextran, pH 7.5). In order to ensure that buffer conditions were properly crowded, a large stock of buffer-A, 1x polymerization buffer, and gelsolin buffer was prepared. Crowded buffer-A, 1x polymerization buffer, and gelsolin buffer was made for each crowded condition. To prepare crowded solution, 10% and 20% weight/weight (w/w) sucrose (292.14 mM and 584.29 mM, respectively) or 3% and 5% w/w PEG (3.75 mM and 6.25 mM, respectively) was weighed out with the final desired weight of the solution set to 10 g. After sucrose or PEG addition, fresh buffer was pulled from the stock and the solution was filled to a final weight of 10 g. The solutions were mixed and stored in 4°C.

2.2 Flow Cell Preparation

Coverslips were sonicated at 60°C in 1 M KOH, followed by 1 M HCl, and finally 70% ethanol for 45 minutes each. Coverslips were thoroughly rinsed with 60°C ddH$_2$O after each sonication step. Silane-PEG MW 2000 and silane-PEG-biotin MW 3400 were purchased from Laysan Bio, Inc. (Arab, AL) 1mg/mL stock solutions of silane-PEG and silane-PEG-biotin were prepared in 80% ethanol and brought to pH ≈2 with HCl. The stock solutions were mixed at ratios ranging from 1:1000 to 1:250 silane-PEG-biotin:silane-PEG. The coverslips were incubated overnight at 60°C in the silane-PEG-biotin:silane-PEG solution, then rinsed with 60°C ddH$_2$O, and dried in a nitrogen stream and stored in a dark, sealed container at 4°C until needed. A flow cell was prepared by placing two strips of double-sided tape lengthwise along the cover glass. A glass slide was adhered to the cover glass (**Fig. 6**). A bovine serum albumin (BSA) and streptavidin solution[65] (5 mg/mL BSA, 100 nM streptavidin in 1x KMI buffer) were loaded onto the flow cell and allowed to incubate for approximately five minutes.

2.3 Total Internal Reflection Fluorescence (TIRF) Microscopy

Actin monomers (2 µM, 25% rhodamine labeled, and 0.07-0.45% biotin labeled) were polymerized at room temperature. For imaging, 0.2mg/mL glucose oxidase, 1mg/mL catalase, and 15 mM glucose were added to the actin sample as a system to reduce photobleaching. Microscopy images were taken with a Nikon Eclipse Ti TIRF microscope equipped with a Hamamatsu ImagEM X2 CCD camera, and a 100x oil immersion objective with a reported pixel size of 0.16 µm/pixel, and a Nikon LU-N4 laser. For steady state experiments 20 images were taken of each slide, and from these images the average filament length as well as the length distribution was

determined. In the time-lapse experiments, images were taken every second. *ImageJ* (NIH) was used to calculate the fraction of unsevered filaments over time.

For the steady state experimentation, actin filaments were polymerized at a concentration of 2 µM (50% rhodamine labeled) for 1 hour in order to reach steady state. Prior to polymerization G-actin was placed in crowded or dilute buffer-A. The crowded buffer concentrations were: 10 and 20% w/w sucrose as well as 3 and 5% w/w PEG. At this point actin was diluted to 1µM and 2.7 nM gelsolin, a 1:370 molar ratio of gelsolin to actin, was added. For crowded samples, the proper concentration crowded gelsolin buffer was used. The sample was mixed and left to incubate for an hour. An hour wait time was needed in order to ensure that the samples imaged were at the end point of the actin-gelsolin interactions. The samples underwent a final 100x dilution and were fixed on coverslips with poly-L-lysine for imaging.

For flow cell imaging, a coverslip was attached to a microscope slide with double sided tape to create a flow chamber (**Fig. 6**). A streptavidin solution[65] (5 mg/mL BSA, 100 nM streptavidin in 1x KMI buffer) was added to the chamber, binding to the biotin fixed to the coverslip. Actin was then polymerized (2 µM 25% rhodamine labeled, 0.07-0.45% biotin labeled) for an hour in dilute or crowded buffer-A, diluted to 200nM, and flowed through the chamber. The biotin tags on the actin filament would then bind and fix the filaments to the silane-PEG-biotin anchors. Once the population of the filaments was deemed adequate, a 1:370 gelsolin to actin molar ratio is added to the chamber in dilute or crowded gelsolin buffer, and images are taken every second to measure the rate of gelsolin severing.

2.4 Steady State and Time-Lapse Image Analysis

Images collected during the steady state experiments were analyzed using ImageJ and *Persistence* software.[66] Only filaments that were sufficiently isolated and in the native shape were analyzed. If two filaments touched each other, or if the filament was looped it was not analyzed. The ends of each filament were selected, and the filament lengths were stored. Data from replications was compiled and statistical analyses were performed using ANOVA one-way[67] and the Scheffe tests[68]. Length distribution of actin filament lengths was plotted. Log-normal (Eq. (1)), Gaussian (Eq. (2)), and double exponential (Eq. (3)) functions were used to fit the data,

$$y = y_0 + \frac{A}{\left(\sqrt{(2\pi)}*w*x\right)} * e^{\left(\frac{-\left(\ln\left(\frac{x}{x_c}\right)\right)^2}{(2*w^2)}\right)} \tag{1}$$

$$y = y_0 + \frac{A}{w\sqrt{\pi/2}} * e^{-2\frac{(x-x_c)^2}{w^2}} \tag{2}$$

$$y = e^{a+bx+cx^2} \tag{3}$$

where w represents log standard deviation or width in Eq. (1) or Eq. (2) respectively and x_c represents the center of distribution.

For time lapse imaging, the first image collected was used to identify all of the filaments that met the same criteria as the steady state filaments, which were isolated and not looped. The time after t_0 that each filament severed was determined and the respective time to severing recorded. The number of unsevered filaments at each time point was divided by the original number of filaments. This produced a steady decreasing value for the fraction of unsevered

filaments that could then be plotted versus time.[51] Finally an exponential decay curve was fit to each line according to Eq. (4)

$$y = y_0 + A_1 * e^{\left[\frac{-(x-x_0)}{t_1}\right]} \tag{4}$$

where t_1 is the time constant, which is inversely proportional to the severing rate can be determined.

2.5 SDS-PAGE Gel Preparation

Bio-Rad Mini-PROTEAN Tetrad glass/short plates were used for hand casting 8.3 cm x 7.3 cm SDS-PAGE gels (Bio-Rad, USA). The resolving gel acrylamide concentration was 12%, which was poured first in the casting apparatus. The acrylamide stock solution used was 40% 37.5:1 Acrylamide-Bis-solution (Bio-Rad, USA). The SDS-PAGE gel solutions were prepared in a 50 mL conical tube. The 12% (v/v) acrylamide resolving gel consisted of: 30% (v/v) 40% acrylamide-bis, 1% (v/v) ammonium persulfate, 0.2% (v/v) TEMED, 1% (v/v) SDS, 0.25M 4x Lower Tris Buffer (pH 8.8), and 42.5% ddH2O. The 6% (v/v) acrylamide stacking gel consisted of: 15% (v/v) 40% acrylamide-bis, 1% (v/v) ammonium persulfate, 0.2% (v/v) TEMED, 1% (v/v) SDS, 0.25M 4x Lower Tris Buffer (pH 8.8), and 58% (v/v) ddH$_2$O.

2.6 Co-sedimentation Assay

Unlabeled actin monomers (5-10 µM) were polymerized in dilute and crowded buffer at room temperature to steady state. Gelsolin (1 µM) was added, the sample was mixed, and left to incubate for 1 hour. Each sample (50 µL) was centrifuged in a Sorvall MTX 150 ultracentrifuge (Thermo Fisher Scientific) using a s100-AT3-2029 rotor (Thermo Fisher Scientific) at 137,900 g for 1 hour at 4°C. After ultracentrifugation, the top 10 µL of the sample was removed as the

supernatant and 10 µL of 1xKMI buffer was added for sucrose samples, while 20 µL 1x KMI buffer was added to the PEG samples. The middle ~30 µL was removed as waste, and the pellet was resuspended with 20 µL of 1x KMI buffer for sucrose samples, and 30 µL of 1x KMI for PEG samples (**Fig. 7**). Dilutions were performed due to the fact that crowded samples ran very poorly though the gel. Samples had 1/10th volume of 4x Laemmli Sample Buffer Dye (25% 1 M Tris-HCl (pH 6.8), 8% (m/V) bromophenol blue (0.1% stock), 20% (m/V) 14.3M B-mercaptoethanol, 40% (m/V) glycerol (100% stock), 5% ddH$_2$O, and 1 g of SDS pellet). Samples were then mixed and incubated in a 100° C water bath for 10 minutes to return the protein to its primary structure.[69] The gel was added to the tank, and electrode buffer was added. Each sample (15 µL) was added to the respective wells and the entire tank was placed on ice, and the gel was run at 80 mV to reduce artifacts produced by the crowders.

After staining and de-staining, the gel was imaged using a Biorad Chemidoc MP imaging system (Biorad, USA). From these images, the adjusted intensity of each band can be used to compare each band relative to a control. For each gel, a control sample of uncrowded actin without gelsolin was run. The intensity from this band was used to normalize all other actin bands. The highest intensity gelsolin band was used to normalize all gelsolin bands. This was done due to the cost of gelsolin. From these normalized values, the gelsolin/F-actin ratio can be calculated for each well, as well as the total amount of actin in the supernatant. Setting the intensity of the actin control band as 100% of the actin, the percent of actin in the supernatant was calculated.

(A)

(B)
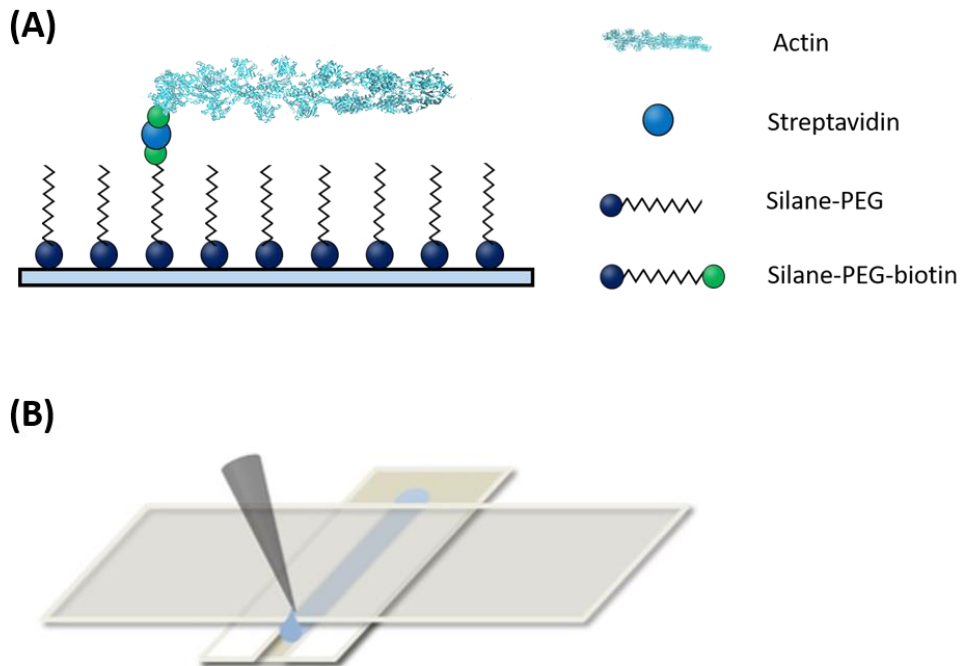
Figure 6: (A) Cartoon representation of our functionalized coverslip. (B) Simple cartoon representation of flow cell construct.

(A) Silane-PEG-biotin is fixed to the surface to act as actin anchors. Silane-PEG spaces these anchors out. Streptavidin can be added to the flow chamber and bind to biotin. Biotin-labeled F-actin can then be added to the chamber and bind to the streptavidin attached to the anchors. All this can be done in the presence of various crowders. (B) The lower glass is the functionalized coverslip and the top glass is a traditional microscope slide.

Co-sedimentation Assay

137,900 g
1 hour

Supernatant

Pellet
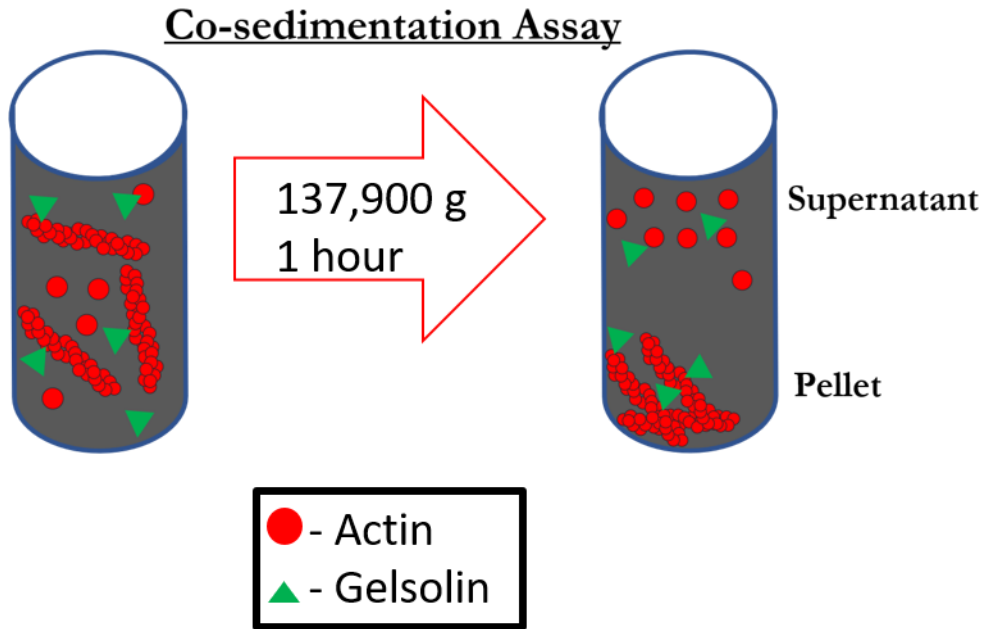
● - Actin
▲ - Gelsolin

Figure 7: **Cartoon representation of co-sedimentation assay used to evaluate gelsolin binding to actin filaments.**

Ultracentrifugation (at 137,900g for 1hr) of samples will pellet the gelsolin bound F-actin, while G-actin and any unbound gelsolin will remain in the supernatant. (Red sphere: actin monomer, green triangle: gelsolin).

CHAPTER THREE: RESULTS AND DISCUSSION

3.1 Gelsolin-Mediated Actin Filament Length Regulation in Crowded Environments

The first goal for this project was to determine if the average filament length and length distribution produced by gelsolin-mediated actin filament severing at equilibrium changes in the presence of macromolecular crowders. Once a filament is in steady state, the actin assembly dynamics reach an equilibrium. This equilibrium affects the average length of actin filaments as well as filament length distribution.[58, 70, 71] Therefore, the steady-state average filament length is considered in order to assess if there is an inhibition or an increase in actin filament severing by ABPs such as cofilin and gelsolin.[58, 72-77] A shorter average filament length generally indicates an increase in severing efficiency, but the length distribution must be calculated and considered in addition to the average filament length. Changes in average actin filament length and length distribution have been linked to altered cellular motility[70] and elasticity[78]. Earlier studies of gelsolin's severing activity were performed using electron microscopy which offered a "snapshot" of the gelsolin and actin interactions.[58] Fluorescence microscopy was also used to track the effect gelsolin severing had on the average actin filament length over time.[58] Other studies have focused on determining how the environment gelsolin is present in affects its function.[79, 80] The dependence of severing activity on Ca^{2+} concentration was determined by studying actin filament lengths produced after gelsolin interactions.[79] The length distribution of actin polymerized in the presence of gelsolin was compared to the distribution of filaments formed with other capping proteins.[80]

There is some debate in the actin biophysics field about which distribution model best describes actin filament length distribution. A previous study had predicted that actin filament

length distribution presented a double exponential distribution[70] in the presence of short range interactions, while other models have found Gaussian distribution to best fit the data.[81] In addition, a recent study by Castaneda et al. found that the actin filament lengths in crowded conditions produce a log-normal distribution.[48] Understanding how the gelsolin-regulated average filament length and filament length distribution are changed in the presence of crowding can help identify the differences in gelsolin function caused by crowded environments.

We first evaluated the effect of crowding on gelsolin-mediated actin filament severing by calculating the average filament length (L_{avg}) imaged using TIRF microscopy (**Fig 8**). Addition of gelsolin (at the molar ratio of 1:370) shortened the average filament lengths ($L_{avg,control} = 4.52 \pm 0.08\,\mu m$, $L_{avg,gelsolin} = 2.80 \pm 0.05\,\mu m$) (**Fig. 9**). 10% w/w sucrose resulted in a significant decrease of the average filament length ($L_{avg} = 3.02 \pm 0.08\,\mu m$) in the absence of gelsolin compared to the control. When gelsolin was added to the sample, a greater decrease in L_{avg} to $2.50 \pm 0.05\,\mu m$ was observed. This decrease of half a micrometer was deemed statistically significant ($p \leq 0.001$) using the Scheffe test. The 20% w/w sucrose sample showed very little difference in the average filament length despite the presence or lack of gelsolin. Actin alone measured $L_{avg} = 2.80 \pm 0.07\,\mu m$, while actin filaments with gelsolin produced an average filament length of $L_{avg} = 2.83 \pm 0.07\,\mu m$. These results indicate that the average filament length generated by gelsolin mediated severing is modulated in the presence of sucrose and is dependent upon sucrose concentration. The fact that 10% w/w and 20% w/w sucrose caused different effects on the average filament length generated by gelsolin severing may be explained by different conformations of actin being more likely in the 10% w/w sucrose sample than in the 20% w/w sucrose sample.

When F-actin was incubated with gelsolin in PEG, a different trend was produced. Actin filaments in buffer with 3% w/w PEG led to $L_{avg} = 3.54 \pm 0.07$ µm. When gelsolin was also present in the solution, there was a decrease in average filament length to $L_{avg} = 2.95 \pm 0.05$ µm. Actin filaments polymerized in crowded buffer containing 5% w/w PEG presented a $L_{avg} = 3.21 \pm 0.06$ µm, which was reduced to $L_{avg} = 2.42 \pm 0.03$ µm when in the presence of gelsolin. The average filament lengths resulting from gelsolin severing in PEG crowded conditions followed a similar trend to the 10% w/w sucrose sample. The average length of the filaments was significantly lowered in the presence of PEG and gelsolin.

Initially, we analyzed the percent change between samples with and without gelsolin. We found that the uncrowded control sample underwent a 38.07% decrease in average filament length when gelsolin was present in solution. In all crowded conditions, except 20% w/w sucrose, gelsolin severing produced a roughly 20% decrease, or half of the percent change in average filament length compared to the control (**Table 1**). The exception to this was seen in samples crowded with 20% w/w sucrose, which showed no difference in average filament length despite the presence of gelsolin. The percent change data may not be the best way to analyze the effect of gelsolin severing as both crowder and gelsolin alone lead to statistically significant shortening of actin filaments. This means that the average filament length in each sample is caused by a combination of crowder shortening filaments[48] and gelsolin severing. Due to this it is difficult to determine how much of the reduction in average filament length is caused by gelsolin severing. However, when considering the average length produced in our samples by gelsolin, we found that there is moderate variation in the average filament length, across most of the crowded conditions. The longest average filament length produced by gelsolin severing was $L_{avg} = 2.95 \pm 0.05$ µm in the

3% w/w PEG sample which is our outlier, while the shortest average length was $L_{avg} = 2.42 \pm 0.03$ µm in the 5% w/w PEG sample. Statistical analysis was performed to compare the differences between the average filament lengths produced by gelsolin severing. We found that the average length of the 3% w/w PEG crowded samples were significantly different to 10% w/w sucrose ($p \leq 0.001$) and 5% w/w PEG ($p \leq 0.001$) samples. We also found that the average filament length produced by 20% w/w sucrose and 5% w/w PEG crowded samples to be significantly different ($p \leq 0.01$). The different effects of sucrose and PEG may be attributed to the difference in size, structure, and polarity of crowders.[82, 83, 84, 85] This change in steady-state filament lengths with crowders suggest that crowding modulates gelsolin's severing activity.

Using the same data as above, we calculated the length distribution of the actin filaments with varying crowding conditions (**Fig. 10**). The distribution of actin filaments in the control sample was very wide, which is traditionally reported.[58] When filaments were in the presence of either crowder, the width of length distribution decreased slightly with the greatest effect observed in the presence of 5% w/w PEG. With the addition of gelsolin all samples showed a further narrowing of the length distribution. To fit the data, we used log-normal, Gaussian, and double exponential distribution functions (see Chapter 2 for details) (**Fig. 10**). Due to the fact that there is not general agreement in the literature, and that the length distribution of actin changes due to ABPs[81], we fit the data using each distribution function to determine which of these methods best fit the length distribution. Among the three fitting functions, log-normal distribution (**Supplemental Table 1**) consistently fits the length distribution better than Gaussian (**Supplemental Table 2**) or double exponential fitting (**Supplemental Table 3**). While the data best fits a log-normal distribution, it still fits very well into Gaussian distribution, which gives us

the ability to measure the narrowing of the distribution caused by crowders and gelsolin by analyzing the change in width (*w*) (**Supplemental Table 2**). There is a very clear trend of decreasing width with increasing crowder concentration and, when gelsolin is added, the decrease in width is exacerbated. The 20% w/w sucrose sample showed very little difference in the average filament length with the addition of gelsolin, however, the length distribution after gelsolin incubation did change, gelsolin further reduced the width of the length distribution of actin filaments in the sample. When gelsolin and actin were incubated in 5% w/w PEG buffer, the decrease in the width of the distribution is relatively small.

Steady state analysis of filaments in crowded conditions with gelsolin allowed us to determine how crowders affect the average filament length and the filament length distribution controlled by gelsolin severing. Our results suggest that gelsolin produces similar average filament lengths in most of our crowded conditions (**Fig. 9)** while there is some difference between sucrose and PEG samples. Sucrose is smaller, has a lower molecular weight, and has higher polarity (calculated by polar surface area) than PEG.[84, 85] The number of molecules in the sucrose crowded solutions was also far greater than the number of crowding molecules present in the PEG crowded solutions (see Chapter 2 for molar concentrations). This difference in the number of crowder molecules may also have an effect on gelsolin activity. Determining the effect of crowding on gelsolin's F-actin severing activity is difficult to conclude from the average filament length data alone. The gelsolin-mediated length distribution narrowed with increasing crowder concentrations (**Fig. 10**). The best fit for the length data was a log-normal distribution, but by using Gaussian distribution it is possible to measure the narrowing of the distributions, with 5% w/w PEG causing the most narrow length distribution (**Supplemental Table 1**).

Both average filament length and length distribution are very important to the function of a cell. Decreases in the average filament length can lead to deficiencies in the elastic properties of the cell.[78] Changes in the length distribution can also effect the elastic properties of the cell, while causing perturbations to the viscoelastic properties that control migration.[70] Understanding the underlying mechanisms that generate force for cellular migration offers insight into processes such as cancer metastasis[86] and wound healing[87].
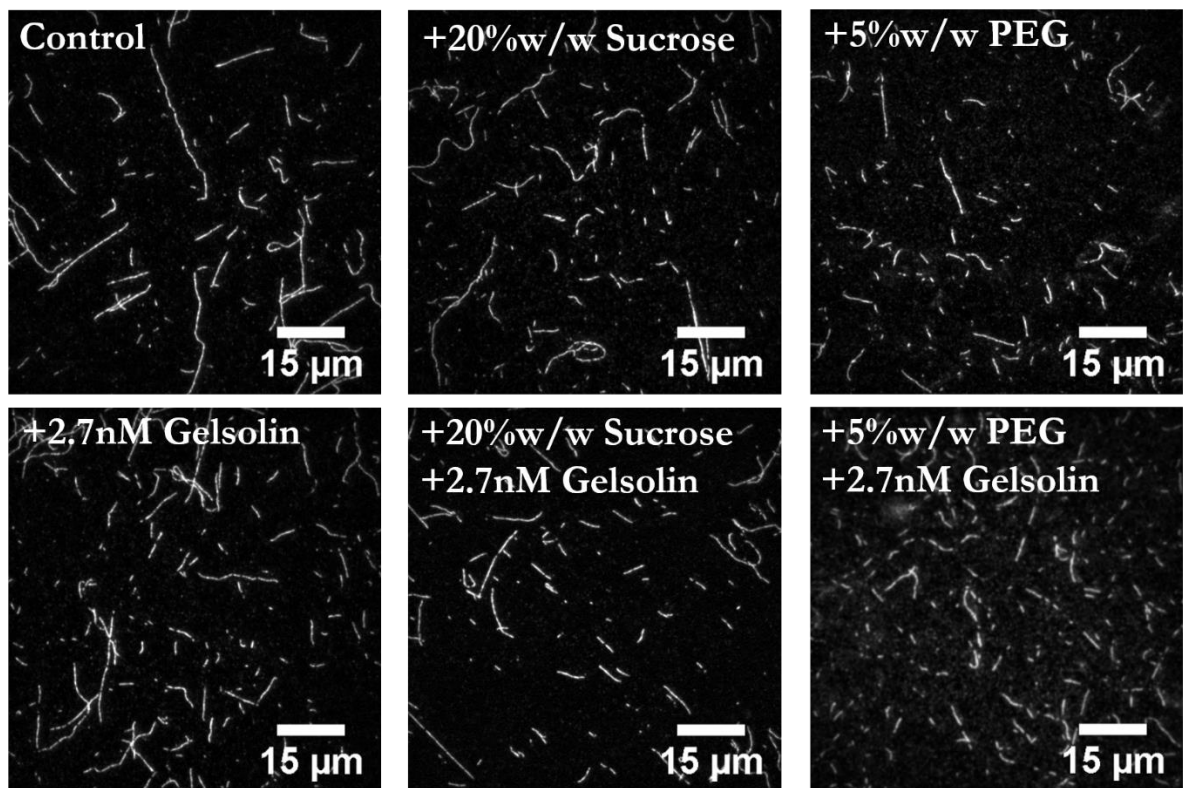
Figure 8: Representative TIRF microscopy images of F-actin in crowded environments without and with gelsolin.

Rhodamine-labeled actin filaments (1 µM) in the absence (top) and presence (bottom) of gelsolin (2.7 nM) at varying crowding conditions. Buffer 10 mM imidazole, pH 7.0, 50 mM KCl, 2 mM MgCl$_2$, 0.2 mM CaCl$_2$, 1 mM ATP, 1 mM DTT with additional 20% w/w sucrose or 5% w/w PEG. (Scale bars, 15 µm).
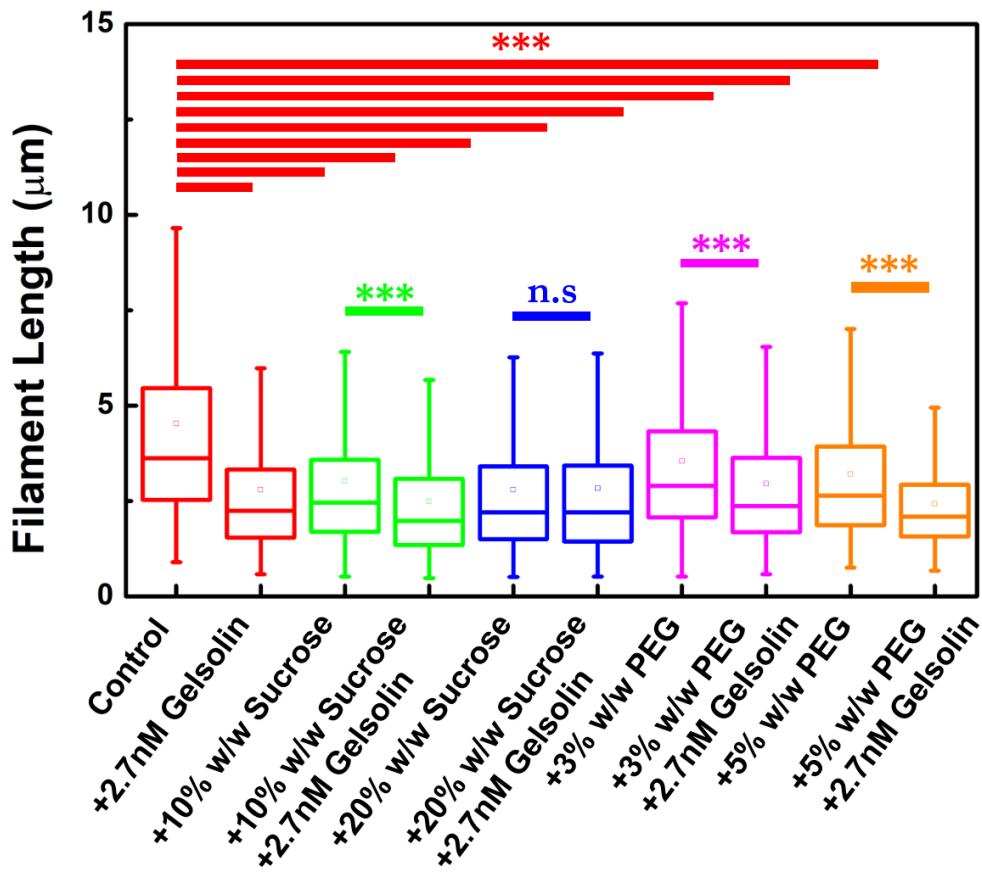
Figure 9: Box plot of steady state actin filament lengths in various crowded conditions with and without gelsolin.

Samples alternate between being incubated in the absence and presence of gelsolin. Buffer: 10 mM imidazole, pH 7.0, 50 mM KCl, 2 mM $MgCl_2$, 0.2 mM $CaCl_2$, 1 mM ATP, 1 mM DTT with additional sucrose or PEG as depicted. Lower and upper whiskers indicate the quartile groups 1 and 4 respectively, while the lower and upper boxes indicate quartile group 2 and 3 respectively. The solid horizonal tile represents the median, and the hollow box the mean. Statistical analysis was performed using the Scheffe test ($N = 644$-2076, n.s.: not significant, ***: $p \leq 0.001$).

Sample	Control	10% w/w Sucrose	20% w/w Sucrose	3% w/w PEG	5% w/w PEG
Percent Change of L_{avg} (%)	38.07	17.43	1.02	16.64	24.63

Table 1: The percent change in average actin filament length (L_{avg}) after the addition of gelsolin in various crowding conditions.

Buffer: 10 mM imidazole, pH 7.0, 50 mM KCl, 2 mM $MgCl_2$, 0.2 mM $CaCl_2$, 1 mM ATP, 1 mM DTT with additional sucrose or PEG as depicted.
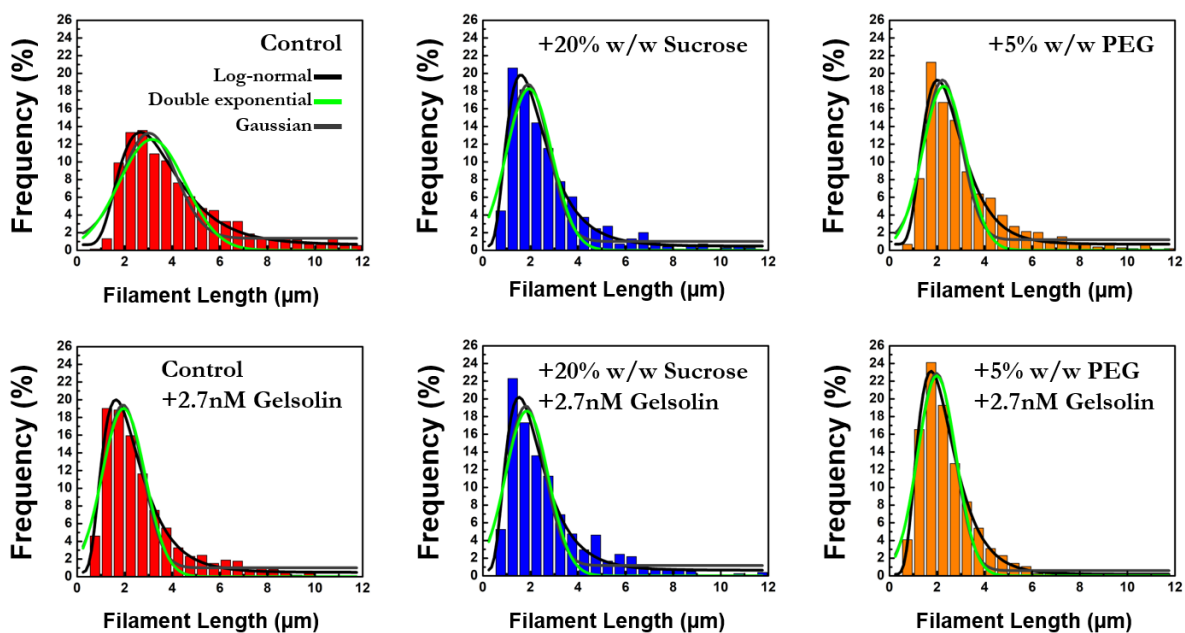
Figure 10: Length distributions of actin filaments in crowded environments without and with gelsolin.

F-actin (1µM) in various crowded conditions in the absence (top) and presence (bottom) of gelsolin (2.7nM). Buffer: 10 mM imidazole, pH 7.0, 50 mM KCl, 2 mM MgCl$_2$, 0.2 mM CaCl$_2$, 1 mM ATP, 1 mM DTT with additional sucrose or PEG as depicted. The fit used was log normal fit (solid black line), Gaussian fit (solid gray line), and double exponential fit (solid green line) according to Eq. (1), (2), and (3) respectively.

3.2 Time-Lapse Imaging of Gelsolin-Mediated Actin Filament Severing in Crowded Environments

The result shown in the previous section (3.1) has helped support the notion that crowding affects gelsolin severing activity, however it is difficult to determine if the severing activity is increased or decreased in the presence of crowders. It is important to determine the effect that macromolecular crowding has on the rate of gelsolin-mediated filament severing. Studies by other groups have tracked the real-time severing activity of ABPs such as cofilin and demonstrated that mechanical or torsional stress enhances cofilin-mediated severing.[51, 76, 77] Comparing the real-time severing activity of gelsolin in crowded conditions to that in dilute conditions will allow us to understand how macromolecular crowding affects relative gelsolin-mediated filament severing rates.

To evaluate the effects of crowding on gelsolin-mediated actin filament severing rates, we directly visualized filament severing in real time by utilizing a functionalized flow cell (**Fig. 6**).[65] Biotinylated F-actin was added to the flow cell, and once the population of the filaments was deemed adequate, gelsolin (at the molar ratio of 1:370 gelsolin to actin) was added to the chamber, and images were taken every second to measure the rate of gelsolin severing (**Fig. 11**). While initially performing this experiment, our goal was to measure the change in average filament length over time. This method proved less than ideal due to problems in accurately measuring the filament length as filaments moved in the z-range. Instead, we calculated the number of unsevered filaments over time.[51] At the beginning of the experiment ($\Delta t = 0$ s) the fraction of unsevered filaments is set to 1, because this is the time point when gelsolin is added to the chamber. As gelsolin severs filaments the fraction of unsevered filaments decreases with each severing event until it reaches 0.

The fraction of unsevered filaments can be calculated for each second of the experiment by determining the number of unsevered filaments at that time divided by the original number of unsevered filaments at 0 s. The decreased fraction of unsevered filaments was plotted on a graph, and an exponential decay function was used to fit the data (**Fig. 12**). From the decay, the t_1, or time constant, value can be determined. t_1 is inversely proportional to the severing rate.

Once the data was collected and the exponential decay curves fit to the data, we were able to compare the relative rate of gelsolin severing in dilute and crowded conditions. We found that the control had the smallest decay time constant (**Fig. 13**), suggesting the highest severing rate. When 10% w/w sucrose was used as a crowder, we saw a slight decrease in the severing rate which was further decreased by the addition of sucrose to a concentration of 20% w/w. The PEG samples did not follow the same trend. When the sample was crowded by 3% w/w PEG, the slowest severing rate was reported. Interestingly, when the amount of crowder was increased to 5% w/w PEG the severing rate of gelsolin actually increased. Compared to control 5% w/w PEG caused the second largest reduction in gelsolin severing rate. Furthermore, PEG had a greater effect on gelsolin mediated severing rate than sucrose. One possible explanation is that sucrose and PEG cause different conformational changes to F-actin or gelsolin, leading to different effects of gelsolin-mediated severing. Overall, this experiment demonstrated that crowding decreased gelsolin-mediated filament severing activity, and the polymeric crowder PEG had a much greater effect than sucrose. This trend is similar to the filament length distribution modulated by both sucrose and PEG (**Fig. 10**), which shows the effect of PEG is greater than sucrose.

This finding indicates that gelsolin-mediated actin filament severing events occur less often in crowded environments. The mechanism for this decrease in severing rate is not currently known,

but we have two potential explanations. The first possibility is that the crowders decrease the rate of gelsolin flown through the chamber, thus increasing the time it takes for gelsolin to travel through the flow cell[88] which would decrease the interactions between gelsolin and actin. The second possibility is that the conformational changes to actin filaments[48] brought on by the crowders reduce the rate of filament severing. The actual mechanism causing the decrease in gelsolin-mediated severing rates is potentially combination of decreased flow rate of gelsolin and conformational changes to actin filaments in the presence of crowders[48]. There is also a possibility that crowded conditions induce conformational changes to gelsolin structure, however this has not been studied yet. Crowding conditions likely vary in different parts of the cell[88-90] and have been shown to decrease the diffusion rate of proteins. With this in mind, crowding could be used by the cell as another tool to control the rate of actin turnover during actin mediated processes, such as force generation for migration.
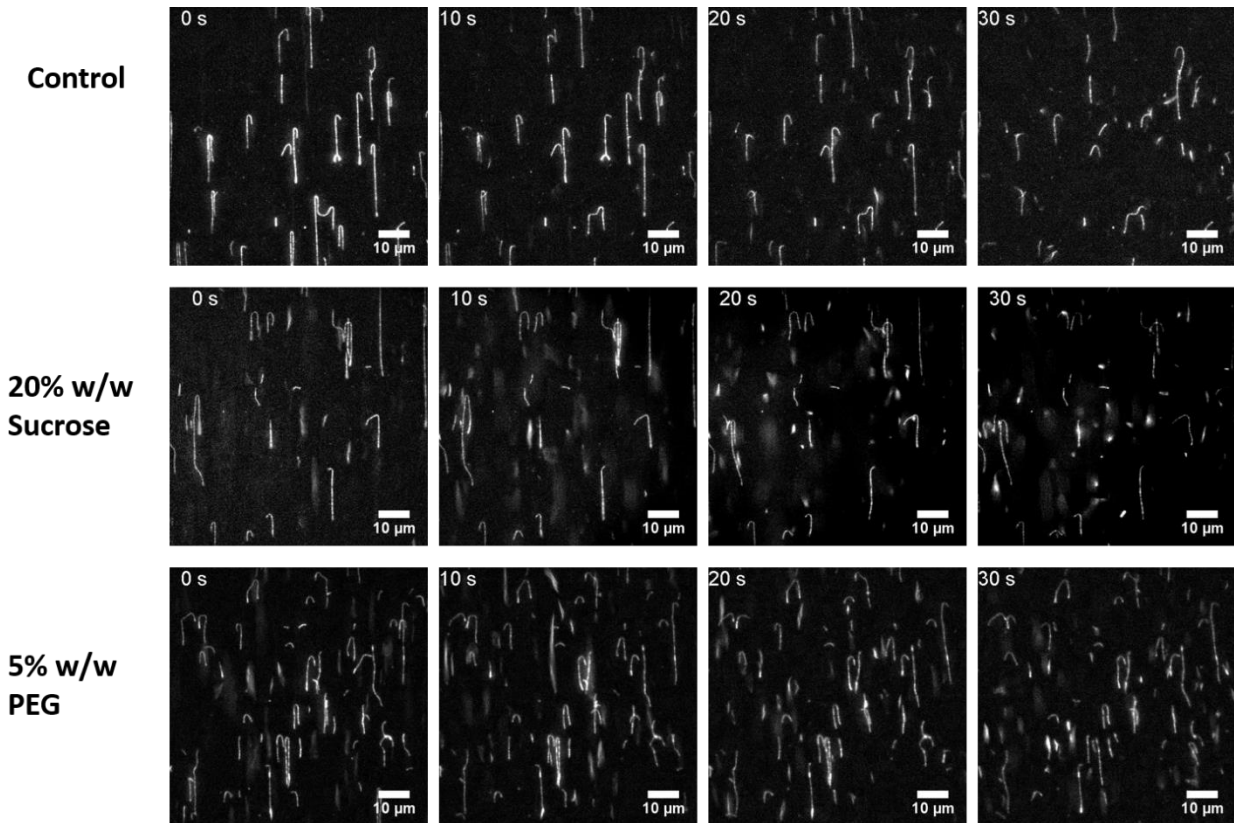
Figure 11: Representative time-lapse TIRF images of gelsolin mediated actin filament severing.

Actin filaments (200 nM, 25% rhodamine labeled, 0.07-0.45% biotinylated) were tethered onto the functionalized coverslip. Gelsolin (0.54 nM) was flowed into a flow cell at t = 0 s. Buffer: 10 mM imidazole, pH 7.0, 50 mM KCl, 2 mM $MgCl_2$, 0.2 mM $CaCl_2$, 1 mM ATP, 1 mM DTT with additional sucrose or PEG as depicted. (Δt = 10 s) (Scale bars, 10 μm).
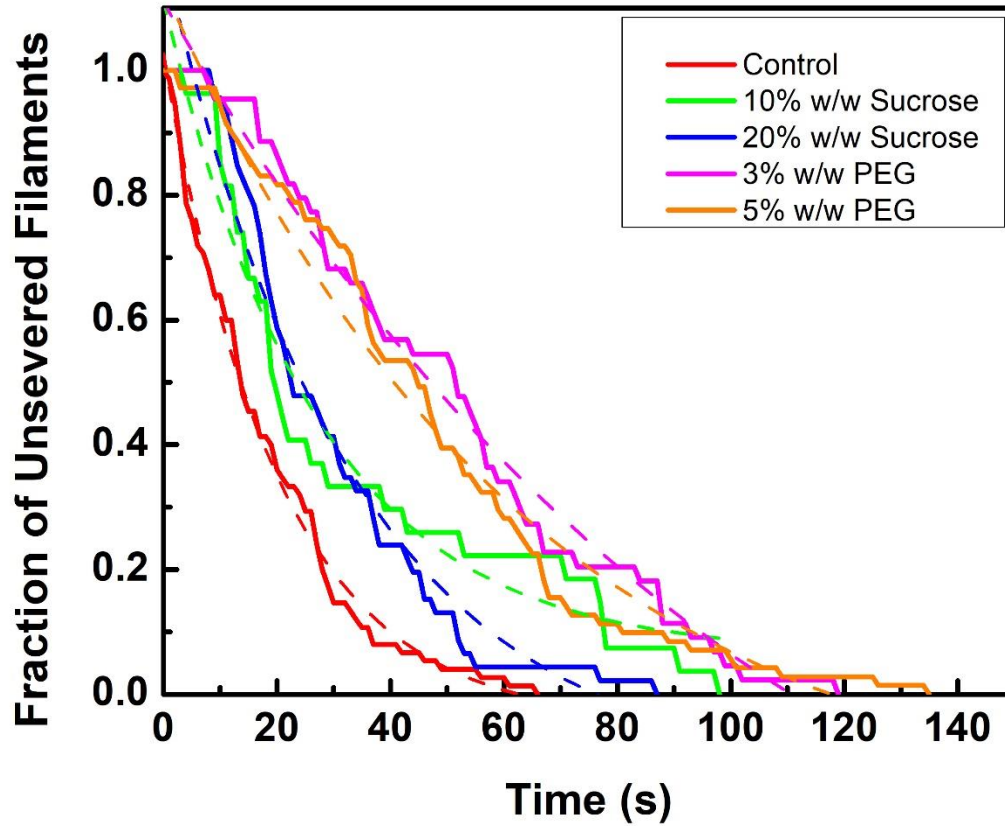
Figure 12: Graphical representation of the fraction of unserved filaments over time at various crowded conditions.

Exponential decay function (Eq. 4) was used to fit the data. Colored dashed lines represent the best fits to data of that color, yielding decay time constant t_1 ($N = 27\text{-}75$).
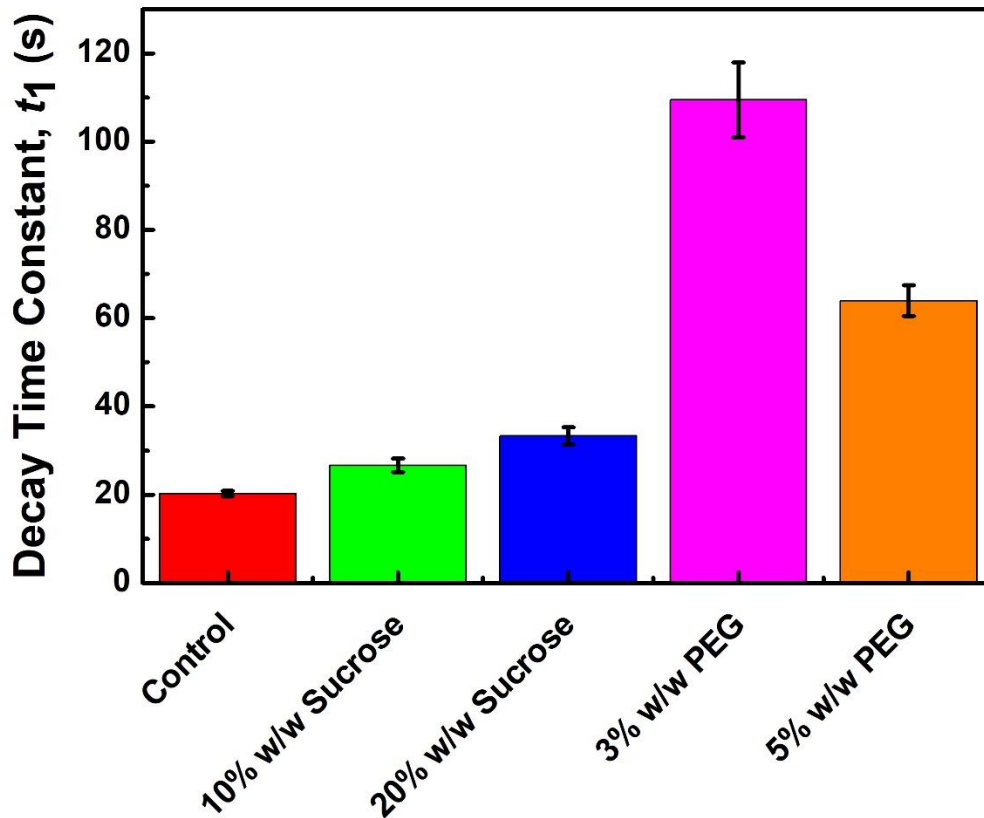
Figure 13: Bar graph of decay time constant, t_1 of gelsolin-mediated filament severing obtained from exponential fitting shown in Figure 12.

Buffer: 10 mM imidazole, pH 7.0, 50 mM KCl, 2 mM $MgCl_2$, 0.2 mM $CaCl_2$, 1 mM ATP, 1 mM DTT with additional sucrose or PEG as depicted. Uncertainty bars represent standard error of the mean (S.E.M.).

3.3 The Effect of Crowding on Gelsolin Binding to F-Actin

Gelsolin binds the barbed-end of F-actin with a very high affinity[29, 59] in dilute buffers ($K_d < 10^{-11}$ M). The ability for gelsolin to bind actin is important, as decreases in gelsolin-actin binding are associated with a reduction in gelsolin severing.[59, 91] Gelsolin binding to actin is controlled by various environmental factors such as pH[91] and Ca^{2+} concentration[59]. However, the binding of gelsolin to actin filaments (F-actin) in the presence of molecular crowders has not been studied yet. Here, we examined changes in the amount of gelsolin bound to F-actin in dilute and crowded conditions by co-sedimentation assays. Co-sedimentation assays utilize ultracentrifugation to separate proteins based on weight. For the case of this experiment, we separated gelsolin bound actin filaments from actin monomers and unbound gelsolin. After centrifugation, the supernatant and pellet were run on SDS-PAGE gels and analyzed **(Fig. 14)**. By plotting a gelsolin/actin ratio for each pellet, we can see, relatively, how much gelsolin is bound to the F-actin in various conditions.

Analysis of SDS-PAGE gels showed that the amount of gelsolin bound to F-actin was reduced in the presence of both crowders **(Fig. 15)**. 10% w/w sucrose resulted in a statistically significant decrease (~50%) in the amount of gelsolin bound to F-actin compared to dilute buffer condition (or control) **(Fig. 15)**. When the amount of sucrose was increased to 20% w/w, there was a recovery of the amount of gelsolin bound to actin almost to the value of the control. When the sample was crowded with 3% w/w PEG, there was a slight, non-significant decrease in the amount of gelsolin bound to actin. When the PEG concentration was further increased to 5% w/w PEG, a significant decrease (~40%) is seen at a similar level of gelsolin bound to actin in the 10% w/w sucrose sample. One concentration of both sucrose and PEG crowded samples caused statistically

significant changes to the amount of gelsolin bound to actin. This is interesting because only the lower concentration sucrose sample caused a significant decrease in the gelsolin to actin ratio while only the higher concentration PEG caused significant changes. This may be caused by actin or gelsolin adopting different conformations depending on the concentration and structure of the crowders. The steady-state length analysis and real-time severing results both agree with the trend found here: PEG has a greater effect on gelsolin-mediated actin severing than sucrose.

By comparing the amount of monomeric actin in the supernatant between samples, the relative severing activity of an actin severing protein can be assessed.[60, 92] In the case of our study, the more actin found in the supernatant, the greater the severing activity of gelsolin. Using this principle, the gels were again analyzed. The first well contained the supernatant actin in dilute buffer without gelsolin, while the third well had gelsolin added. As shown in **(Fig. 14)**, both wells had very little actin present. Gelsolin severing is not expected to disassemble actin in dilute buffer conditions, but is expected to sever and cap, thus, creating shorter filaments. This is why we did not see an increase in the amount of monomeric actin with the addition of gelsolin. If more monomeric actin is found in crowded conditions, we can conclude that an increase severing activity of gelsolin and filament disassembly is the cause.

Interestingly, increasing concentration of crowders increased the amount of actin in the supernatant. Initially, in the sample crowded with 10% w/w sucrose we saw no real difference in the amount of monomeric actin in the supernatant, i.e., about 1% of the actin was in the supernatant **(Fig. 16)**. Once the sucrose concentration was increased to 20% w/w, there was a statistically significant ($P \leq 0.05$) increase in the amount of monomeric actin compared to the 10% w/w sucrose sample, which presented as a 3.21 ± 0.61 % increase. The PEG crowded samples showed a much

greater effect. When F-actin and gelsolin were crowded by 3% w/w PEG, there was a significant increase in the amount of G-actin, $6.71 \pm 1.79\%$ of the actin was non-filamentous. This percentage was further increased to $12.41 \pm 1.11\%$ G-actin in the 5% w/w PEG sample. Both sucrose and PEG caused increases in the severing activity of gelsolin, but only PEG caused statistically significant increases in the amount of monomeric actin compared to the control. This again demonstrates the variation in effects caused by crowders of different size and structure.

One interpretation of these results is that the molecular crowders are causing this increase in the amount of monomeric actin due to changes in the critical concentration[93, 94], thus causing filament disassembly. To study this a gel was run with samples of PEG crowded actin with and without gelsolin (**Fig. 17**). This gel revealed that there is no difference in the amount of monomeric actin between actin in dilute or crowded conditions. This leaves us to interpret that the increase in monomeric actin in crowded gelsolin solutions is produced by an increase in gelsolin-mediated filament severing due to the crowders.[95]

The results drawn from the co-sedimentation assays seem to be contradictory due to the fact that a decrease in gelsolin binding to F-actin (**Fig. 15**) is expected to be accompanied by a decrease in gelsolin severing activity. It has been found that macromolecular crowding, specifically by sucrose and PEG, induces conformational changes of actin filaments.[48] Different structural states of filaments modulate binding interactions of gelsolin segment 1 (s1), a fragment of gelsolin that can sever and bind to the barbed end of F-actin in a Ca^{2+} dependent manner.[52] Based on these studies, we speculate that crowders alter the conformation of F-actin in a way that weakens or disrupts gelsolin binding at the barbed end of the actin filament. This weakened binding offers the opportunity for the gelsolin cap to disassociate from the barbed end of the actin filament,

allowing it to sever another filament(s). This would lead to greater disassembly of actin filaments due to gelsolin severing multiple times in crowded buffers, something that would not occur in dilute buffer conditions. This altered binding would also explain the differences in the amount of gelsolin bound to F-actin.
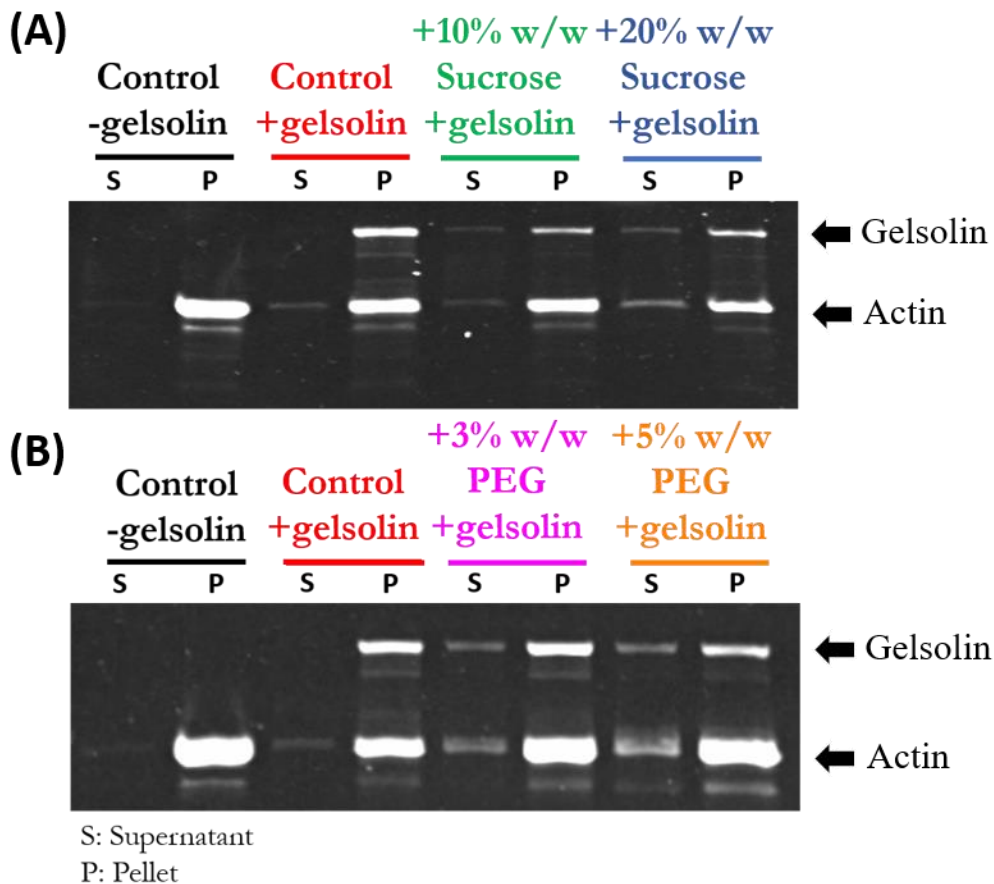
Figure 14: Representative SDS-PAGE gel images of co-sedimentation samples.

The gels were imaged by Biorad Chemidoc. Actin (5-10 µM) alone or actin and gelsolin (1 µM) were incubated together for 1 hour in dilute or crowded buffers. (S: supernatant, P: Pellet). Buffer: 10 mM imidazole, pH 7.0, 50 mM KCl, 2 mM $MgCl_2$, 0.2 mM $CaCl_2$, 1 mM ATP, 1 mM DTT with additional sucrose (A) or PEG (B) as depicted.
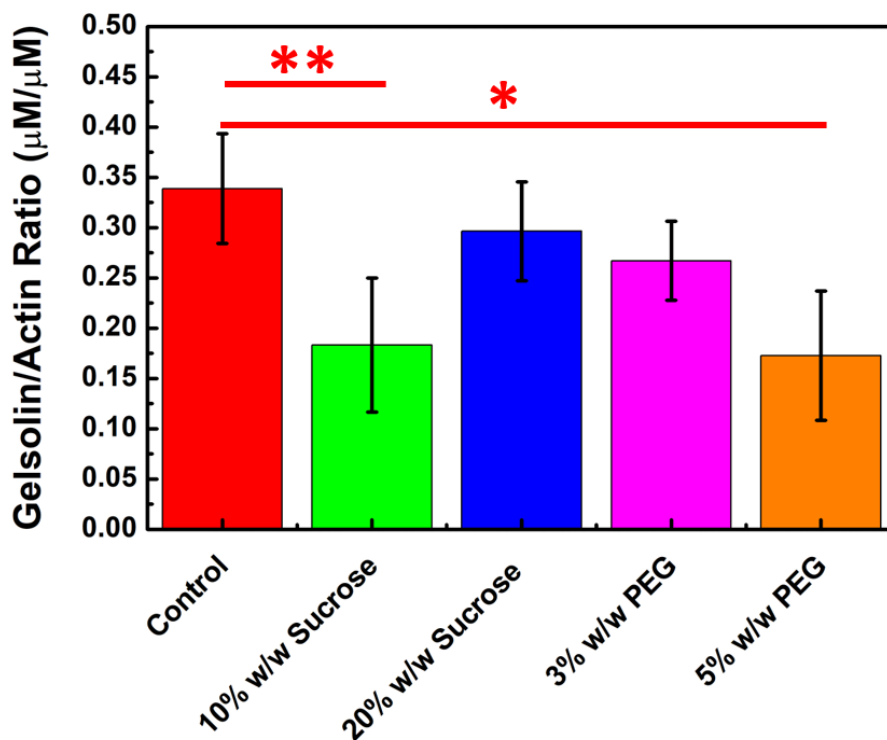
Figure 15: Bar graph representing the molar ratio between gelsolin and actin analyzed from SDS-PAGE gel images.

Actin and gelsolin were incubated together for 1 hour in dilute or crowded buffers. Buffer: 10 mM imidazole, pH 7.0, 50 mM KCl, 2 mM $MgCl_2$, 0.2 mM $CaCl_2$, 1 mM ATP, 1 mM DTT with additional sucrose or PEG as depicted. Uncertainty bars represent standard deviation (S.D.). Statistical analysis was performed using the Scheffe test ($N = 3$-5, *: $p \leq 0.05$ **: $p \leq 0.01$).
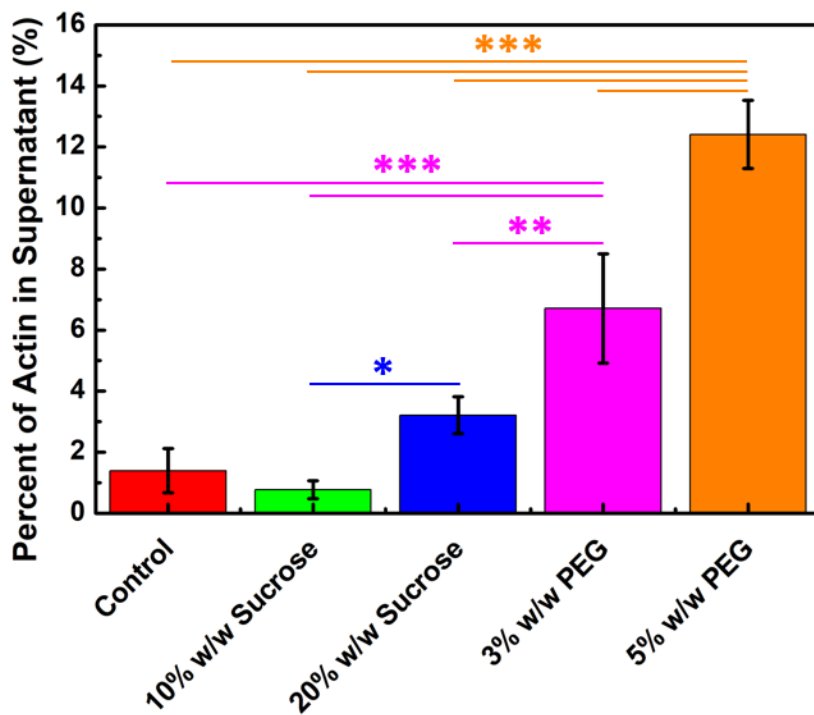
Figure 16: Bar graph representation of the percent of actin in the supernatant.

The percent of actin was determined using the Biorad gel image intensities. Actin and gelsolin were incubated together for 1 hour in dilute or crowded buffers. Buffer: 10 mM imidazole, pH 7.0, 50 mM KCl, 2 mM $MgCl_2$, 0.2 mM $CaCl_2$, 1 mM ATP, 1 mM DTT with additional sucrose or PEG as depicted. Uncertainty bars represent standard deviation (S.D.). Statistical analysis was performed using the Scheffe test ($N = 3\text{-}5$, *: $p \leq 0.05$ **: $p \leq 0.01$ ***: $p \leq 0.001$).
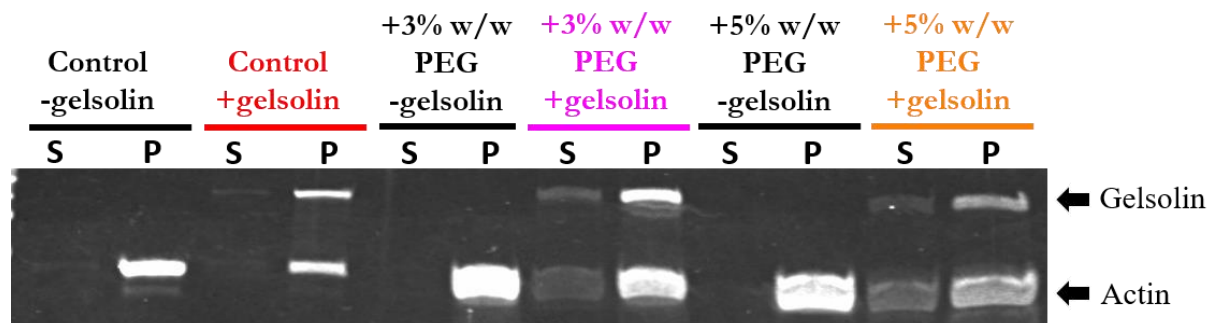
Figure 17: Representative SDS-PAGE gel image of co-sedimentation samples without and with gelsolin.

The gel was imaged by Biorad Chemidoc. Actin (5 µM) and gelsolin (1 µM) or actin alone was incubated for 1 hour in dilute or crowded buffers. (S: supernatant, P: Pellet) Buffer: 10 mM imidazole, pH 7.0, 50 mM KCl, 2 mM $MgCl_2$, 0.2 mM $CaCl_2$, 1 mM ATP, 1 mM DTT with additional sucrose or PEG as depicted.

CHAPTER FOUR: CONCLUSIONS

When studying various human diseases, it is critical to understand the interactions between proteins that function within the cellular space. Until recently, the crowded environment of the intracellular space was not considered when characterizing protein-protein interactions and function. This omission can lead to misunderstandings of how proteins function. When considering Familial Amyloidosis, Finnish type (FAF), the conformation, activity, and availability of gelsolin are critical to understanding the disease state.[96] Studying proteins in the presence of macromolecular crowders offers researchers the opportunity to analyze protein interactions in conditions that better model the physiological environment and conformation these proteins exist in.

The results presented in this study demonstrate how different our understanding of gelsolin and actin interactions may be from what is actually occurring inside the cell. We know that crowding induces conformational changes to F-actin[48] and have shown in this study that crowding also alters gelsolin-actin binding interactions and gelsolin's severing activity. In a crowded environment the end point average filament length (**Fig. 9**) has some variation but understanding the effect of crowding on gelsolin's severing activity was difficult to determine. The length distribution of actin filaments produced by gelsolin in the presence of crowders is narrower compared to the distribution generated by gelsolin in dilute conditions (**Fig. 10**). This may have an effect on cellular function by altering cellular motility[70] and elasticity[78]. We have also shown that the relative severing rate of gelsolin is reduced in all crowded samples tested (**Fig. 13**), which has large implications because much of the prior rate data about gelsolin severing has been

determined in dilute buffer conditions.[56, 74] We have demonstrated that in crowded conditions there is less gelsolin bound to F-actin (**Fig. 15**), which is accompanied by an increase in monomeric actin in the supernatant (**Fig. 16**). Cofilin, another severing protein, also has its severing activity and binding affected when F-actin undergoes a conformational change and becomes over-twisted.[50, 51] We speculate that due to the changes in F-actin conformation generated by crowding, and potential changes to gelsolin conformation, the binding of gelsolin to the barbed end of actin filaments can be altered. This alteration may allow the gelsolin cap to disassociate from the barbed end of the filament, allowing it to sever more than once. While proving this hypothesis is outside the scope of this work, disassociation of gelsolin from the barbed end of F-actin without cellular signals can have meaningful implications into how researchers understand gelsolin activity inside living cells. It could shift the paradigm from gelsolin being a one and done severing protein to a more dynamic player, which dissociates from the barbed end of F-actin and retains its ability to sever more filaments.

Throughout this work it has been demonstrated that sucrose and PEG often cause different magnitudes of effects on gelsolin's actin severing activity. In the time-lapse imaging we see PEG causing a greater decrease in the severing rate of gelsolin than sucrose (**Fig. 13**). We also see a much greater increase in gelsolin severing activity as evidenced by the amount of monomeric actin in PEG crowded samples compared to sucrose crowded samples (**Fig. 16**). When considering the effect of crowders on the amount of gelsolin bound to F-actin we see opposite trends when comparing sucrose crowded and PEG crowded samples. Only low concentration sucrose causes a significant decrease in the gelsolin/actin ratio while only high concentration PEG causes a significant decrease (**Fig. 15**). These differences in effects can be explained by the different

structures of each crowder. Sucrose is a smaller molecule, more polar, and at the concentrations used there were many more sucrose molecules than PEG molecules.[82, 84, 85] The molar concentration of the 10% and 20% w/w sucrose crowded samples was 292.14 mM and 584.29 mM respectively, while the molar concentration of the 3% and 5% PEG crowded samples was 3.75 mM and 6.25mM respectively. The difference in molar concentration illustrates the large disparity in the number of sucrose molecules and PEG molecules present in the crowded solutions. Another important difference between the two crowders is that PEG is a polymeric macromolecule therefore much larger than sucrose, whereas sucrose is a monomeric crowder.[83] The simple difference in the number of molecules and size may affect protein-protein interactions with different magnitudes in crowded solutions. Additionally PEG induces a greater excluded volume effect than sucrose,[48] partially explaining the varying results. Potential differences in induced conformational changes to actin and gelsolin caused by either crowder could also change the results obtained from our crowded samples. Finally differences in the viscosity of the crowded solutions may have slowed or changed our gelsolin-actin interactions.

There are a few directions this work can move in from this point. While it is clear that molecular crowders have an effect on protein function, it is also clear that the structure and size of the crowder are characteristics that partially dictate the magnitude of those effects. As this study has shown, sucrose and PEG behave differently, generally PEG has a greater effect on gelsolin function. Because of this, studying inert macromolecules that are biologically relevant individually, followed by studies with these crowders in combination would prove useful. Determining the conformation of gelsolin and F-actin in the presence of crowders is another potential direction for future work. Molecular dynamics simulations could be performed along

with experimental biophysics and biochemistry studies to further support the findings. Finally, studying gelsolin's capping and uncapping at the barbed end of actin filaments in crowded conditions would support or refute our proposed alteration of the gelsolin-F-actin binding. Using inert molecular crowders to model the intracellular space gives researchers the opportunity to study disease related proteins in relative isolation. This has the potential to aid in drug target research, as the conformation and activity of the target should be similar to physiological conditions.

APPENDIX A-
SUPPLEMENTAL INFORMATION

Supplemental Table 1: Values of the parameters used in log-normal fitting (Eq. 1) to the filament length data in Figure 11.

Log-Normal fitting	Offset (Y_0)	Center (x_c)	Log standard deviation	Area (a)	Adjusted R^2
Control	0.64 ±0.30	3.27 ±0.08	0.45 ±.026	42.43 ±1.84	0.965
+2.7nM Gelsolin	0.49 ±0.20	2.07 ±0.04	0.49 ±0.02	44.07 ±1.21	0.965
+10% Sucrose	0.32 ±0.30	2.30 ±0.06	0.50 ±0.03	46.22 ±1.84	0.971
+10% Sucrose +2.7nM Gelsolin	0.53 ±0.28	1.82 ±0.05	0.51 ±0.02	43.65 ±1.68	0.974
+20% Sucrose	0.48 ±0.31	2.05 ±0.06	0.51 ±0.03	44.25 ±1.85	0.968
+20% Sucrose +2.7nM Gelsolin	0.64 ±0.39	1.95 ±0.07	0.50 ±0.03	42.31 ±2.30	0.948
+3% w/w PEG	0.41 ±0.25	2.76 ±0.06	0.47 ±0.02	45.13 ±1.54	0.978
+3% w/w PEG +2.7nM Gelsolin	0.53 ±0.22	2.23 ±0.04	0.47 ±0.02	43.70 ±1.34	0.982
+5% w/w PEG	0.69 ±0.33	2.39 ±0.06	0.41 ±0.02	41.69 ±1.97	0.959
+5% w/w PEG +2.7nM Gelsolin	0.18 ±0.11	2.11 ±0.02	0.43 ±0.01	47.88 ±0.64	0.997

Supplemental Table 2: Values of the parameters used in Gaussian fitting (Eq. 2) to the filament length data in Figure 11.

Gaussian Fitting	Offset (Y_0)	Center (x_c)	Width (w)	Area (a)	Adjusted R^2
Control	1.36 ±0.49	3.03 ±0.12	2.27 ±0.27	33.81 ±4.19	0.843
+2.7nM Gelsolin	1.01 ±0.48	1.92 ±0.07	1.66 ±0.16	38.28 ±3.51	0.899
+10% Sucrose	0.89 ±0.54	2.13 ±0.09	1.87 ±0.20	39.76 ±4.23	0.871
+10% Sucrose +2.7nM Gelsolin	1.13 ±0.58	1.64 ±0.08	1.47 ±0.16	36.93 ±3.97	0.863
+20% Sucrose	1.00 ±0.58	1.90 ±0.09	1.73 ±0.20	38.46 ±4.36	0.853
+20% Sucrose +2.7nM Gelsolin	1.17 ±0.62	1.80 ±0.09	1.61 ±0.20	36.38 ±4.49	0.827
+3% w/w PEG	1.05 ±0.50	2.55 ±0.10	2.07 ±0.22	37.66 ±4.07	0.871
+3% w/w PEG +2.7nM Gelsolin	1.12 ±0.50	2.05 ±0.08	1.65 ±0.16	36.76 ±3.61	0.885
+5% w/w PEG	1.21 ±0.54	2.23 ±0.08	1.57 ±0.17	35.58 ±3.79	0.868
+5% w/w PEG +2.7nM Gelsolin	0.60 ±0.41	1.98 ±0.05	1.54 ±0.11	43.05 ±2.86	0.944

Supplemental Table 3: Values of the parameters used in Gaussian fitting (Eq. 3) to the filament length data in Figure 11.

Double exponential fitting	Coefficient (A)	Coefficient (B)	Coefficient (C)	Adjusted R^2
Control	-0.02 ±0.52	1.62 ±0.34	-0.26 ±0.05	0.802
+2.7nM Gelsolin	0.61 ±0.42	2.39 ±0.43	-0.61 ±0.11	0.883
+10% Sucrose	0.60 ±0.44	2.09 ±0.41	-0.48 ±0.10	0.861
+10% Sucrose +2.7nM Gelsolin	0.95 ±0.45	2.46 ±0.54	-0.73 ±0.15	0.847
+20% Sucrose	0.83 ±0.45	2.14 ±0.47	-0.55 ±0.12	0.841
+20% Sucrose +2.7nM Gelsolin	0.82 ±0.51	2.28 ±0.55	-0.62 ±0.14	0.809
+3% w/w PEG	0.27 ±0.46	1.87 ±0.36	-0.36 ±0.07	0.853
+3% w/w PEG +2.7nM Gelsolin	0.32 ±0.49	2.48 ±0.47	-0.59 ±0.11	0.865
+5% w/w PEG	-0.32 ±0.65	2.84 ±0.58	-0.62 ±0.12	0.845
+5% w/w PEG +2.7nM Gelsolin	0.08 ±0.39	3.06 ±0.39	-0.77 ±0.10	0.941

APPENDIX B-
COPYRIGHT PERMISSIONS

This Agreement between University of Central Florida -- James Heidings ("You") and Elsevier ("Elsevier") consists of your license details and the terms and conditions provided by Elsevier and Copyright Clearance Center.

License Number	4804940555315
License date	Apr 09, 2020
Licensed Content Publisher	Elsevier
Licensed Content Publication	Elsevier Books
Licensed Content Title	International Review of Cytology
Licensed Content Author	Shoichiro Ono
Licensed Content Date	Jan 1, 2007
Licensed Content Pages	82
Start Page	1
End Page	82
Type of Use	reuse in a thesis/dissertation

This Agreement between University of Central Florida -- James Heidings ("You") and Elsevier ("Elsevier") consists of your license details and the terms and conditions provided by Elsevier and Copyright Clearance Center.

License Number	4804960365860
License date	Apr 09, 2020
Licensed Content Publisher	Elsevier
Licensed Content Publication	Biochimica et Biophysica Acta (BBA) - General Subjects
Licensed Content Title	Size-dependent studies of macromolecular crowding on the thermodynamic stability, structure and functional activity of proteins: in vitro and in silico approaches
Licensed Content Author	Sumra Shahid,Md. Imtaiyaz Hassan,Asimul Islam,Faizan Ahmad
Licensed Content Date	Feb 1, 2017
Licensed Content Volume	1861
Licensed Content Issue	2
Licensed Content Pages	20
Start Page	178
End Page	197
Type of Use	reuse in a thesis/dissertation

This Agreement between University of Central Florida -- James Heidings ("You") and Elsevier ("Elsevier") consists of your license details and the terms and conditions provided by Elsevier and Copyright Clearance Center.

License Number	4804950734011
License date	Apr 09, 2020
Licensed Content Publisher	Elsevier
Licensed Content Publication	The International Journal of Biochemistry & Cell Biology
Licensed Content Title	Flightless I: An actin-remodelling protein and an important negative regulator of wound repair
Licensed Content Author	Z. Kopecki,A.J. Cowin
Licensed Content Date	Jan 1, 2008
Licensed Content Volume	40
Licensed Content Issue	8
Licensed Content Pages	5
Start Page	1415
End Page	1419
Type of Use	reuse in a thesis/dissertation

This Agreement between University of Central Florida -- James Heidings ("You") and Elsevier ("Elsevier") consists of your license details and the terms and conditions provided by Elsevier and Copyright Clearance Center.

License Number	4804941036609
License date	Apr 09, 2020
Licensed Content Publisher	Elsevier
Licensed Content Publication	Structure
Licensed Content Title	Near-Atomic Resolution for One State of F-Actin
Licensed Content Author	Vitold E. Galkin,Albina Orlova,Matthijn R. Vos,Gunnar F. Schröder,Edward H. Egelman
Licensed Content Date	Jan 6, 2015
Licensed Content Volume	23
Licensed Content Issue	1
Licensed Content Pages	10
Start Page	173
End Page	182
Type of Use	reuse in a thesis/dissertation

REFERENCES

1.   Dou, Y.; Arlock, P.; Arner, A., Blebbistatin specifically inhibits actin-myosin interaction in mouse cardiac muscle. *Am. J. Physiol. Cell Physiol.* **2007,** *293* (3), C1148-C1153.
2.   Pollard, T. D.; Cooper, J. A., Actin, a Central Player in Cell Shape and Movement. *Science (New York, N.Y.)* **2009,** *326* (5957), 1208-1212.
3.   Small, J. V.; Stradal, T.; Vignal, E.; Rottner, K., The lamellipodium: where motility begins. *Trends Cell Biol.* **2002,** *12* (3), 112-120.
4.   May, R. C.; Machesky, L. M., Phagocytosis and the actin cytoskeleton. *J. Cell Sci.* **2001,** *114* (6), 1061-1077.
5.   Mogilner, A.; Oster, G., Cell motility driven by actin polymerization. *Biophy. J.* **1996,** *71* (6), 3030-3045.
6.   Casella, J. F.; Flanagan, M. D.; Lin, S., Cytochalasin D inhibits actin polymerization and induces depolymerization of actin filaments formed during platelet shape change. *Nature* **1981,** *293* (5830), 302-305.
7.   Levee, M. G.; Dabrowska, M. I.; J. L. Lelli, J.; Hinshaw, D. B., Actin polymerization and depolymerization during apoptosis in HL-60 cells. *Am. J. Physiol. Cell Physiol.* **1996,** *271* (6), 1981-1992.
8.   Gourlay, C. W.; Ayscough, K. R., The actin cytoskeleton in ageing and apoptosis. *FEMS Yeast Res.* **2005,** *5* (12), 1193-1198.
9.   Dominguez, R.; Holmes, K. C., Actin Structure and Function. *Annu. Rev. Biophys.* **2011,** *40* (1), 169-186.
10.   Pollard, T. D.; Cooper, J. A., Actin and actin-binding proteins. A critical evaluation of mechanisms and functions. *Annu. Rev. Biochem.* **1986,** *55*, 987-1035.
11.   and, H. N. H.; Pollard, T. D., Regulation of Actin Filament Network Formation Through ARP2/3 Complex: Activation by a Diverse Array of Proteins. *Annu. Rev. Biochem.* **2001,** *70* (1), 649-676.
12.   Pollard, T. D.; Blanchoin, L.; Mullins, R. D., Molecular Mechanisms Controlling Actin Filament Dynamics in Nonmuscle Cells. *Annu. Rev. Biophys. Biomol. Struct.* **2000,** *29* (1), 545-576.
13.   Tang, D. D.; Gerlach, B. D., The roles and regulation of the actin cytoskeleton, intermediate filaments and microtubules in smooth muscle cell migration. *Respir. Res.* **2017,** *18*, 54.
14.   Webb, D. J.; Parsons, J. T.; Horwitz, A. F., Adhesion assembly, disassembly and turnover in migrating cells -- over and over and over again. *Nat. Cell Biol.* **2002,** *4* (4), 97-100.
15.   Crevenna, A. H.; Naredi-Rainer, N.; Schönichen, A.; Dzubiella, J.; Barber, D. L.; Lamb, D. C.; Wedlich-Söldner, R., Electrostatics control actin filament nucleation and elongation kinetics. *J. biol. Chem.* **2013,** *288* (17), 12102-12113.
16.   Wang, F.; Sampogna, R. V.; Ware, B. R., pH dependence of actin self-assembly. *Biophys. J.* **1989,** *55* (2), 293-298.
17.   Kang, H.; Bradley, M. J.; McCullough, B. R.; Pierre, A.; Grintsevich, E. E.; Reisler, E.; De La Cruz, E. M., Identification of cation-binding sites on actin that drive polymerization and modulate bending stiffness. *Proc. Natl. Acad. Sci. U. S. A.* **2012,** *109* (42), 16923-16927.
18.   Senger, R.; Goldmann, W. H., The influence of cations and ionic strength on actin polymerization in the presence/absence of alpha-actinin. *Biochem. Mol. Biol. Int.* **1995,** *35* (1), 103-109.
19.   Pollard, T. D., Regulation of actin filament assembly by Arp2/3 complex and formins. *Annu. Rev. Biophys. Biomol. Struct.* **2007,** *36*, 451-477.
20.   Meggs, L. G.; Tillotson, J.; Huang, H.; Sonnenblick, E. H.; Capasso, J. M.; Anversa, P., Noncoordinate regulation of alpha-1 adrenoreceptor coupling and reexpression of alpha skeletal actin in myocardial infarction-induced left ventricular failure in rats. *J. Clin. Invest.* **1990,** *86* (5), 1451-1458.

21.   Stanton, L. W.; Garrard, L. J.; Damm, D.; Garrick, B. L.; Lam, A.; Kapoun, A. M.; Zheng, Q.; Protter, A. A.; Schreiner, G. F.; White, R. T., Altered Patterns of Gene Expression in Response to Myocardial Infarction. *Circ. Res.* **2000,** *86* (9), 939-945.

22.   Goebel, H. H.; Anderson, J. R.; Hübner, C.; Oexle, K.; Warlo, I., Congenital myopathy with excess of thin myofilaments. *Neuromuscul. Disord.* **1997,** *7* (3), 160-168.

23.   Nowak, K. J.; Wattanasirichaigoon, D.; Goebel, H. H.; Wilce, M.; Pelin, K.; Donner, K.; Jacob, R. L.; Hübner, C.; Oexle, K.; Anderson, J. R.; Verity, C. M.; North, K. N.; Iannaccone, S. T.; Müller, C. R.; Nürnberg, P.; Muntoni, F.; Sewry, C.; Hughes, I.; Sutphen, R.; Lacson, A. G.; Swoboda, K. J.; Vigneron, J.; Wallgren-Pettersson, C.; Beggs, A. H.; Laing, N. G., Mutations in the skeletal muscle α-actin gene in patients with actin myopathy and nemaline myopathy. *Nat. Genet.* **1999,** *23* (2), 208-212.

24.   Chan, C.; Fan, J.; Messer, A. E.; Marston, S. B.; Iwamoto, H.; Ochala, J., Myopathy-inducing mutation H40Y in ACTA1 hampers actin filament structure and function. *Biochim. Biophys. Acta.* **2016,** *1862* (8), 1453-1458.

25.   Clarke, N. F.; Ilkovski, B.; Cooper, S.; Valova, V. A.; Robinson, P. J.; Nonaka, I.; Feng, J. J.; Marston, S.; North, K., The pathogenesis of ACTA1-related congenital fiber type disproportion. *Ann. Neurol.* **2007,** *61* (6), 552-561.

26.   Kwiatkowski, D. J., Functions of gelsolin: motility, signaling, apoptosis, cancer. *Curr. Opin. Cell Biol.* **1999,** *11* (1), 103-108.

27.   Harris, H. E.; Weeds, A. G., Plasma gelsolin caps and severs actin filaments. *FEBS Lett.* **1984,** *177* (2), 184-188.

28.   Li, G. H.; Arora, P. D.; Chen, Y.; McCulloch, C. A.; Liu, P., Multifunctional roles of gelsolin in health and diseases. *Med. Res. Rev.* **2012,** *32* (5), 999-1025.

29.   Janmey, P. A.; Chaponnier, C.; Lind, S. E.; Zaner, K. S.; Stossel, T. P.; Yin, H. L., Interactions of gelsolin and gelsolin-actin complexes with actin. Effects of calcium on actin nucleation, filament severing, and end blocking. *Biochemistry* **1985,** *24* (14), 3714-3723.

30.   Janmey, P. A.; Stossel, T. P., Modulation of gelsolin function by phosphatidylinositol 4,5-bisphosphate. *Nature* **1987,** *325* (6102), 362-364.

31.   Grazi, E.; Magri, E.; Cuneo, P.; Cataldi, A., The control of cellular motility and the role of gelsolin. *FEBS Lett.* **1991,** *295* (1-3), 163-166.

32.   Cooper, J. A.; Loftus, D. J.; Frieden, C.; Bryan, J.; Elson, E. L., Localization and mobility of gelsolin in cells. *J. Cell Bio.* **1988,** *106* (4), 1229-1240.

33.   Cunningham, C.; Stossel, T.; Kwiatkowski, D., Enhanced motility in NIH 3T3 fibroblasts that overexpress gelsolin. *Science (New York, N.Y.)* **1991,** *251* (4998), 1233-1236.

34.   Witke, W.; Sharpe, A. H.; Hartwig, J. H.; Azuma, T.; Stossel, T. P.; Kwiatkowski, D. J., Hemostatic, inflammatory, and fibroblast responses are blunted in mice lacking gelsolin. *Cell* **1995,** *81* (1), 41-51.

35.   Li, G. H.; Shi, Y.; Chen, Y.; Sun, M.; Sader, S.; Maekawa, Y.; Arab, S.; Dawood, F.; Chen, M.; De Couto, G.; Liu, Y.; Fukuoka, M.; Yang, S.; Da Shi, M.; Kirshenbaum, L. A.; McCulloch, C. A.; Liu, P., Gelsolin regulates cardiac remodeling after myocardial infarction through DNase I-mediated apoptosis. *Circ. Res.* **2009,** *104* (7), 896-904.

36.   de la Cuesta, F.; Zubiri, I.; Maroto, A. S.; Posada, M.; Padial, L. R.; Vivanco, F.; Alvarez-Llamas, G.; Barderas, M. G., Deregulation of smooth muscle cell cytoskeleton within the human atherosclerotic coronary media layer. *J. Proteomics* **2013,** *82*, 155-165.

37.   Haltia, M.; Prelli, F.; Ghiso, J.; Kiuru, S.; Somer, H.; Palo, J.; Frangione, B., Amyloid protein in familial amyloidosis (Finnish type) is homologous to gelsolin, an actin-binding protein. *Biochem. Biophys. Res. Commun.* **1990,** *167* (3), 927-932.

38.	Kothakota, S.; Azuma, T.; Reinhard, C.; Klippel, A.; Tang, J.; Chu, K.; McGarry, T. J.; Kirschner, M. W.; Koths, K.; Kwiatkowski, D. J., Caspase-3-generated fragment of gelsolin: effector of morphological change in apoptosis. *Science (New York, N.Y.)* **1997,** *278* (5336), 294-298.

39.	Nishio, R.; Matsumori, A., Gelsolin and Cardiac Myocyte Apoptosis. *Circ. Res.* **2009,** *104* (7), 829-831.

40.	Hosek, M.; Tang, J. X., Polymer-induced bundling of F actin and the depletion force. *Phys. Rev. E* **2004,** *69* (5), 051907.

41.	Cino, E. A.; Karttunen, M.; Choy, W.-Y., Effects of molecular crowding on the dynamics of intrinsically disordered proteins. *PLoS One* **2012,** *7* (11), e49876.

42.	Cheung, M. S.; Thirumalai, D., Effects of crowding and confinement on the structures of the transition state ensemble in proteins. *J. Phys. Chem. B* **2007,** *111* (28), 8250-8257.

43.	Ellis, R. J.; Minton, A. P., Cell biology: join the crowd. *Nature* **2003,** *425* (6953), 27-28.

44.	Minton, A. P., The influence of macromolecular crowding and macromolecular confinement on biochemical reactions in physiological media. *J. Biol. Chem.* **2001,** *276* (14), 10577-10580.

45.	Rosin, C.; Schummel, P. H.; Winter, R., Cosolvent and crowding effects on the polymerization kinetics of actin. *Phys. Chem. Chem. Phys.* **2015,** *17* (13), 8330-8337.

46.	De La Cruz, E. M.; Pollard, T. D., Nucleotide-Free Actin: Stabilization by Sucrose and Nucleotide Binding Kinetics. *Biochemistry* **1995,** *34* (16), 5452-5461.

47.	Gagarskaia, I. A.; Povarova, O. I.; Uversky, V. N.; Kuznetsova, I. M.; Turoverov, K. K., The effects of crowding agents Dextran-70k and PEG-8k on actin structure and unfolding reaction. *J. Mol. Struct.* **2017,** *1140*, 46-51.

48.	Castaneda, N.; Lee, M.; Rivera-Jacquez, H. J.; Marracino, R. R.; Merlino, T. R.; Kang, H., Actin Filament Mechanics and Structure in Crowded Environments. *J. Phys. Chem. B* **2019,** *123* (13), 2770-2779.

49.	De La Cruz, E. M.; Roland, J.; McCullough, B. R.; Blanchoin, L.; Martiel, J. L., Origin of twist-bend coupling in actin filaments. *Biophys. J.* **2010,** *99* (6), 1852-1860.

50.	Schramm, A. C.; Hocky, G. M.; Voth, G. A.; Blanchoin, L.; Martiel, J.-L.; De La Cruz, E. M., Actin Filament Strain Promotes Severing and Cofilin Dissociation. *Biophys. J.* **2017,** *112* (12), 2624-2633.

51.	Wioland, H.; Jegou, A.; Romet-Lemonne, G., Torsional stress generated by ADF/cofilin on cross-linked actin filaments boosts their severing. *Proc. Natl. Acad. Sci.* **2019,** *116* (7), 2595-2602.

52.	Lee, M.; Kang, E. H., Molecular dynamics study of interactions between polymorphic actin filaments and gelsolin segment-1. *Proteins Struct. Funct. Bioinf.* **2020,** *88* (2), 385-392.

53.	Minton, A.; Wilf, J., Effect of macromolecular crowding upon the structure and function of an enzyme: glyceraldehyde-3-phosphate dehydrogenase. *Biochemistry* **1981,** *20* (17), 4821-4826.

54.	Yang, J.; Moravec, C. S.; Sussman, M. A.; DiPaola, N. R.; Fu, D.; Hawthorn, L.; Mitchell, C. A.; Young, J. B.; Francis, G. S.; McCarthy, P. M., Decreased SLIM1 expression and increased gelsolin expression in failing human hearts measured by high-density oligonucleotide arrays. *Circulation* **2000,** *102* (25), 3046-3052.

55.	Zorgati, H.; Larsson, M.; Ren, W.; Sim, A. Y. L.; Gettemans, J.; Grimes, J. M.; Li, W.; Robinson, R. C., The role of gelsolin domain 3 in familial amyloidosis (Finnish type). *Proc. Natl. Acad. Sci.* **2019,** *116* (28), 13958-13963.

56.	Allen, P. G.; Janmey, P. A., Gelsolin displaces phalloidin from actin filaments. A new fluorescence method shows that both Ca2+ and Mg2+ affect the rate at which gelsolin severs F-actin. *J. Biol. Chem.* **1994,** *269* (52), 32916-32923.

57.	Bearer, E. L., Direct observation of actin filament severing by gelsolin and binding by gCap39 and CapZ. *J. Cell. Biol.* **1991,** *115* (6), 1629-1638.

58.   Burlacu, S.; Janmey, P. A.; Borejdo, J., Distribution of actin filament lengths measured by fluorescence microscopy. *Am. J. Physiol.* **1992,** *262*, 569-577.

59.   Kinosian, H. J.; Newman, J.; Lincoln, B.; Selden, L. A.; Gershman, L. C.; Estes, J. E., Ca2+ regulation of gelsolin activity: binding and severing of F-actin. *Biophys. J.* **1998,** *75* (6), 3101-3109.

60.   Qian, D.; Nan, Q.; Yang, Y.; Li, H.; Zhou, Y.; Zhu, J.; Bai, Q.; Zhang, P.; An, L.; Xiang, Y., Gelsolin-Like Domain 3 Plays Vital Roles in Regulating the Activities of the Lily Villin/Gelsolin/Fragmin Superfamily. *PloS one* **2015,** *10* (11), e0143174

61.   Galkin, Vitold E.; Orlova, A.; Vos, Matthijn R.; Schröder, Gunnar F.; Egelman, Edward H., Near-Atomic Resolution for One State of F-Actin. *Structure* **2015,** *23* (1), 173-182.

62.   Kopecki, Z.; Cowin, A. J., Flightless I: An actin-remodelling protein and an important negative regulator of wound repair. *Int. J. Biochem. Cell Biol.* **2008,** *40* (8), 1415-1419.

63.   Ono, S., Mechanism of Depolymerization and Severing of Actin Filaments and Its Significance in Cytoskeletal Dynamics. *Int. Rev. Cytol.* **2007**, *258*, 1-82.

64.   Shahid, S.; Hassan, M. I.; Islam, A.; Ahmad, F., Size-dependent studies of macromolecular crowding on the thermodynamic stability, structure and functional activity of proteins: in vitro and in silico approaches. *Biochim. Biophys. Acta Gen. Subj.* **2017,** *1861* (2), 178-197.

65.   Winterhoff, M.; Brühmann, S.; Franke, C.; Breitsprecher, D.; Faix, J., Visualization of actin assembly and filament turnover by in vitro multicolor TIRF microscopy. *Chemotaxis* **2016**, *1407*, 287-306.

66.   Graham, J. S.; McCullough, B. R.; Kang, H.; Elam, W. A.; Cao, W.; De La Cruz, E. M., Multi-platform compatible software for analysis of polymer bending mechanics. *PLoS One* **2014,** *9* (4), e94766.

67.   Weiss, D. J., *Analysis of Variance and Functional Measurement*. Oxford University Press: 2006; p 8-22.

68.   Heiberger, R. M.; Holland, B., *Statistical Analysis and Data Display*. Springer: New York, 2004; p 729.

69.   Gallagher, S. R., One-dimensional SDS gel electrophoresis of proteins. *Curr. Protoc. Mol. Biol.* **2012,** *97* (1), 10.2 A. 1-10.2 A. 44.

70.   Popp, D.; Gov, N. S.; Iwasa, M.; Maéda, Y., Effect of short-range forces on the length distribution of fibrous cytoskeletal proteins. *Biopolymers* **2008,** *89* (9), 711-721.

71.   Sept, D.; Xu, J.; Pollard, T. D.; Andrew McCammon, J., Annealing Accounts for the Length of Actin Filaments Formed by Spontaneous Polymerization. *Biophys. J.* **1999,** *77* (6), 2911-2919.

72.   Xiang, Y.; Huang, X.; Wang, T.; Zhang, Y.; Liu, Q.; Hussey, P. J.; Ren, H., ACTIN BINDING PROTEIN 29 from Lilium pollen plays an important role in dynamic actin remodeling. *Plant Cell* **2007,** *19* (6), 1930-1946.

73.   Pavlov, D.; Muhlrad, A.; Cooper, J.; Wear, M.; Reisler, E., Severing of F-actin by yeast cofilin is pH-independent. *Cell Motil.* **2006,** *63* (9), 533-542.

74.   Dąbrowska, R.; Hinssen, H.; Gałązkiewicz, B.; Nowak, E., Modulation of gelsolin-induced actin-filament severing by caldesmon and tropomyosin and the effect of these proteins on the actin activation of myosin Mg2+-ATPase activity. *Biochem. J.* **1996,** *315* (3), 753-759.

75.   Ishikawa, R.; Yamashiro, S.; Matsumura, F., Differential modulation of actin-severing activity of gelsolin by multiple isoforms of cultured rat cell tropomyosin. Potentiation of protective ability of tropomyosins by 83-kDa nonmuscle caldesmon. *J. Biol. Chem.* **1989,** *264* (13), 7490-7497.

76.   McCullough, Brannon R.; Grintsevich, Elena E.; Chen, Christine K.; Kang, H.; Hutchison, Alan L.; Henn, A.; Cao, W.; Suarez, C.; Martiel, J.-L.; Blanchoin, L.; Reisler, E.; De La Cruz, E. M., Cofilin-Linked Changes in Actin Filament Flexibility Promote Severing. *Biophys. J.* **2011,** *101* (1), 151-159.

77.	Kang, H.; Bradley, M. J.; Cao, W.; Zhou, K.; Grintsevich, E. E.; Michelot, A.; Sindelar, C. V.; Hochstrasser, M.; De La Cruz, E. M., Site-specific cation release drives actin filament severing by vertebrate cofilin. *Proc. Natl. Acad. Sci. U. S. A.* **2014,** *111* (50), 17821-17826.

78.	Biron, D.; Moses, E., The Effect of α-Actinin on the Length Distribution of F-Actin. *Biophys. J.* **2004,** *86* (5), 3284-3290.

79.	Yin, H. L.; Hartwig, J. H.; Maruyama, K.; Stossel, T. P., Ca2+ control of actin filament length. Effects of macrophage gelsolin on actin polymerization. *J. Biol. Chem.* **1981,** *256* (18), 9693-9697.

80.	Kuhlman, P. A., Dynamic changes in the length distribution of actin filaments during polymerization can be modulated by barbed end capping proteins. *Cell Motil.* **2005,** *61* (1), 1-8.

81.	Gov, N. S., Theory of the length distribution of tread-milling actin filaments inside bundles. *Europhys. Lett.* **2007,** *77* (6), 68005.

82.	Miyazawa, T.; Fukushima, K.; Ideguchi, Y., Molecular vibrations and structure of high polymers. III. Polarized infrared spectra, normal vibrations, and helical conformation of polyethylene glycol. *J. Chem. Phys.* **1962,** *37* (12), 2764-2776.

83.	Brown, G. M.; Levy, H. A., Further refinement of the structure of sucrose based on neutron-diffraction data. *Acta Cryst. B* **1973,** *29* (4), 790-797.

84.	Pubchem. https://pubchem.ncbi.nlm.nih.gov/compound/174#section=Computed-Properties (accessed June 10th 2020).

85.	Pubchem. https://pubchem.ncbi.nlm.nih.gov/compound/5988#section=Computed-Properties (accessed June 10th, 2020).

86.	Olson, M. F.; Sahai, E., The actin cytoskeleton in cancer cell motility. *Acta Cryst. B* **2008,** *26* (4), 273-287.

87.	Darby, I.; Skalli, O.; Gabbiani, G., a-Smooth muscle actin is transiently expressed by myofibroblasts during experimental wound healing. *Lab. Invest.* **1990,** *63* (1), 21-29.

88.	Coquel, A.-S.; Jacob, J.-P.; Primet, M.; Demarez, A.; Dimiccoli, M.; Julou, T.; Moisan, L.; Lindner, A. B.; Berry, H., Localization of Protein Aggregation in Escherichia coli Is Governed by Diffusion and Nucleoid Macromolecular Crowding Effect. *PLOS Comput. Biol.* **2013,** *9* (4), e1003038.

89.	Smith, S.; Cianci, C.; Grima, R., Macromolecular crowding directs the motion of small molecules inside cells. *J. R. Soc. Interface* **2017,** *14* (131), 20170047.

90.	Valkenburg, J. A.; Woldringh, C. L., Phase separation between nucleoid and cytoplasm in Escherichia coli as defined by immersive refractometry. *J. Bacteriol.* **1984,** *160* (3), 1151-1157.

91.	Lamb, J.; Allen, P.; Tuan, B.; Janmey, P., Modulation of gelsolin function. Activation at low pH overrides Ca2+ requirement. *J. Biol. Chem.* **1993,** *268* (12), 8999-9004.

92.	Vartiainen, M. K.; Mustonen, T.; Mattila, P. K.; Ojala, P. J.; Thesleff, I.; Partanen, J.; Lappalainen, P., The three mouse actin-depolymerizing factor/cofilins evolved to fulfill cell-type-specific requirements for actin dynamics. *Mol. Biol. Cell* **2002,** *13* (1), 183-194.

93.	Drenckhahn, D.; Pollard, T. D., Elongation of actin filaments is a diffusion-limited reaction at the barbed end and is accelerated by inert macromolecules. *J. Biol. Chem.* **1986,** *261* (27), 12754-12758.

94.	Tellam, R. L.; Sculley, M. J.; Nichol, L. W.; Wills, P., The influence of poly (ethylene glycol) 6000 on the properties of skeletal-muscle actin. *Biochem. J.* **1983,** *213* (3), 651-659.

95.	Huang, S.; Blanchoin, L.; Chaudhry, F.; Franklin-Tong, V. E.; Staiger, C. J., A gelsolin-like protein from Papaver rhoeas pollen (PrABP80) stimulates calcium-regulated severing and depolymerization of actin filaments. *J. Biol. Chem.* **2004,** *279* (22), 23364-23375.

96.	Levy, E.; Haltia, M.; Fernandez-Madrid, I.; Koivunen, O.; Ghiso, J.; Prelli, F.; Frangione, B., Mutation in gelsolin gene in Finnish hereditary amyloidosis. *J. Exp. Med.* **1990,** *172* (6), 1865-1867.